Semianalytical cloud retrieval algorithm as applied to the cloud top altitude and the cloud geometrical thickness determination from top-of-atmosphere reflectance measurements in the oxygen A band

Vladimir V. Rozanov and Alexander A. Kokhanovsky[1]
Institute of Environmental Physics, Bremen University, Bremen, Germany

Received 25 August 2003; revised 16 December 2003; accepted 26 December 2003; published 5 March 2004.

[1] The paper is devoted to the development of the asymptotic algorithm for the cloud top height h and the geometrical thickness l determination using measurements of the cloud reflection function. It is based on the asymptotic theory of the radiative transfer in the oxygen absorption bands and simple parameterization of the radiative transport in the atmosphere above and under a cloud. In particular, we have studied the influence of the error of the developed approximate theory on the accuracy of the retrieval of the pair (h, l). It was assumed that there is only a single cloud layer having the same value of the liquid water content in all points inside the cloud. The values (h, l) have been found, solving the inverse problem having as input the synthetic spectra of backscattered light. The synthetic spectra were found using the exact solution of the forward problem for given values of (h, l). The retrieval technique was based on the asymptotic theory. We have found that the error of the cloud top height determination is smaller than 20 m, and the error of the cloud geometrical thickness determination is smaller than 500 m for solar angles 20–70 degrees, values of h in the range 1–12 km, values of geometrical thickness l in the range 0.5–2 km, and values of the cloud optical thickness changing in the range 10–50. The surface albedo has been assumed to be equal zero. We have also studied the influence of the cloud liquid water profile on the results of the retrieval of the pair (h, l). It was found that the error of the cloud top height determination increases up to 600 m, if the assumed cloud has a changing with height liquid water content, and retrievals are made applying the inversion with assumed constant liquid water content profile. The error in the geometrical thickness increases up to 1 km in this case. Errors of the retrieval increase even further if the retrieval, on the basis of the homogeneous layer theory, is applied to the two-layered cloud system (e.g., the upper cloud consists of ice crystals and the lower cloud is in a liquid phase). This signifies the importance of the cloud vertical inhomogeneity on the retrieval results. *INDEX TERMS:* 0305 Atmospheric Composition and Structure: Aerosols and particles (0345, 4801); 0320 Atmospheric Composition and Structure: Cloud physics and chemistry; 0343 Atmospheric Composition and Structure: Planetary atmospheres (5405, 5407, 5409, 5704, 5705, 5707); 0345 Atmospheric Composition and Structure: Pollution—urban and regional (0305); *KEYWORDS:* radiative transfer, clouds, remote sensing

Citation: Rozanov, V. V., and A. A. Kokhanovsky (2004), Semianalytical cloud retrieval algorithm as applied to the cloud top altitude and the cloud geometrical thickness determination from top-of-atmosphere reflectance measurements in the oxygen A band, *J. Geophys. Res.*, *109*, D05202, doi:10.1029/2003JD004104.

1. Introduction

[2] Cloud altitude and geometrical thickness are important parameters for a number of meteorological and climatological applications. For instance, the very position of a cloud top height may be an indication of an inversion layer in the atmosphere. Cloud altitudes and types indicate the thermodynamic and hydrodynamic structure of the atmosphere. These parameters affect energy budgets and radiative heating. In particular, higher altitudes of clouds lead to higher surface temperatures.

[3] The distribution of heating in the cloud, which is influenced by the cloud top height and the geometrical thickness, is of importance for the cloud dynamics and the evolution of cloud microstructure. Also, cloud top and cloud base heights influence the photon horizontal transport in clouds [*Titov*, 1998]. This has an importance to a number of issues and in particular to a so-called cloud absorption anomaly problem [*Stephens and Tsay*, 1990].

[4] This emphasizes the importance of information on the cloud top height h, the cloud geometrical thickness l, and

[1] Also at Institute of Physics, Minsk, Belarus.

0148-0227/04/2003JD004104$09.00

the cloud base height $b = h - l$ derived on a global scale. Values h and l can be, in principle, retrieved using satellite measurements. A great number of methods has been proposed for the determination of the cloud top height h. They range from active measurements [see, e.g., *Winker et al.*, 1999; *Poole et al.*, 2003], using lidars and radars on satellite platforms, to passive techniques, on the basis of the processing of information, contained in the thermal infrared radiances [*King et al.*, 1992], ring effect [*Joiner and Bhartia*, 1995; *de Beek et al.*, 2001], reflected light polarization [*Knibbe et al.*, 2000], and stereo photogrammetric technique [*Moroney et al.*, 2002], to name a few.

[5] In particular, measured thermal infrared radiances are converted to cloud top pressures using assumed (or known from other sources) an atmospheric temperature profile [*King et al.*, 1992; *Platnick et al.*, 2003]. A possible error in this profile influences the retrieval results considerably [*Naud et al.*, 2002].

[6] Most accurate estimations (the accuracy in h is better than 20 m) can be obtained from satellite laser systems. However, they are rather expensive and have a poor spatial coverage.

[7] A great number of passive techniques developed also indicate that none of them can provide an accuracy comparable with laser active systems. In particular, *Naud et al.* [2002] found that Moderate resolution Imaging Spectroradiometer (MODIS), developed by NASA [*King et al.*, 1992], gives the values of h, which differ from those obtained from the ground-based microwave measurements up to 1–2 km. MODIS data for h can differ from correspondent data obtained from the Multi-Angle Imaging Spectroradiometer (MISR) by 2 km. Note that MODIS low cloud top height product is based on the brightness temperature measured at 11 μm. For high clouds, MODIS algorithm is relied upon the CO_2-slicing method [*King et al.*, 1992]. Then the CO_2 15 μm absorption band is used for the retrieval procedure. The MISR cloud altitude retrievals are derived from multiangle red channel radiances and a stereo photogrammetric technique [*Moroney et al.*, 2002].

[8] Generally, measurements in visible and near-infrared cannot be used to retrieve the parameters h and l. This is due to an extremely weak sensitivity of the top-of-atmosphere radiance I to these parameters in this spectral region. Indeed, the radiative transfer equation, which is usually applied to the interpretation of satellite measurements, has as a parameter the value of the optical thickness τ, which is a product of l and a priori unknown value of the cloud extinction coefficient σ_{ext} (for homogeneous clouds). The value of τ can be easily obtained from measurements in visible [*Nakajima and King*, 1990] or near-infrared [*Platnick et al.*, 2003]. Measurements in near-infrared can be also used to find the effective radius of particles a_{ef} [*Nakajima and King*, 1990; *Nakajima et al.*, 1991; *Kokhanovsky et al.*, 2003] and cloud thermodynamic state [*Knap et al.*, 2002]. However, the information on the parameters h and l is virtually absent. This is actually of a benefit for the retrievals of a_{ef}, τ, and liquid water path W, which is proportional to the product of a_{ef} and τ. Note that it follows approximately:

$$W = A a_{ef} \tau,$$

where $A = 2\rho/3$ and $\rho = 1$ gcm^{-3} is the density of water.

[9] The situation is radically changed if we consider the radiative transfer in the molecular absorption line [*Yamomoto and Wark*, 1961; *Heidinger*, 1998; *Stephens and Heidinger*, 2000; *Heidinger and Stephens*, 2000, 2002]. Indeed, let us assume that we have a gas in a planetary atmosphere, which absorbs almost all incident radiation in a narrow band. Then the depth of this band, measured by a receiver on a satellite, will depend on the cloud altitude. Gas concentrations generally decrease with the distance from the ground. Therefore clouds at a high altitude do not allow photons to penetrate to low atmospheric layers and be absorbed there. So the depth of a molecular line will decrease if high clouds are present in the field of view of a sensor.

[10] This idea for the cloud top height retrieval was proposed by *Hanel* [1961] and has already been applied for cloud top altitude measurements. In particular, *Saiedy et al.* [1967] analyzed measurements obtained by the Gemini5 astronauts in the region of the oxygen A band centered at 760 nm. Measurements were performed using a small handheld spectrograph with the spectral resolution 5 Å or 10 Å, depending on settings. They were able to determine altitude of several cloud systems (e.g., Sc cloud over the east Pacific, a cloud in the Intertropical Convergence Zone, the hurricane Doreen, etc.) [see *Saiedy et al.*, 1967, Table 1]. In particular, the absorption line for the area over a hurricane was not so pronounced as for a case of a low Sc cloud. They found that the hurricane top pressure p was 323 mb ($h \approx 7$ km). The value of p for a Sc cloud was 835 mb ($h \approx 2$ km).

[11] An important finding of their work was the fact that the cloud geometrical thickness l cannot be ignored in the retrieval procedure. *Saiedy et al.* [1967] emphasized that the measured cloud top altitudes, on the basis of the assumption that the cloud is substituted by the Lambertian diffuser with zero transmittance, give values that are always below actual cloud top heights.

[12] This can be easily understood on physical grounds as well. Indeed, in reality photons penetrate through a cloud top in inner cloud areas (and also below a cloud) and are absorbed by oxygen there. This leads to the increase of the oxygen absorption depth even for high clouds. If the process of the photon penetration is neglected (a Lambertian diffuser assumption), then this increased depth of the absorption line is interpreted as an existence of a cloud on a level that is lower that the actual altitude of a cloud. This actually was observed by *Saiedy et al.* [1965] while comparing retrieved cloud top heights (from airborne reflectance spectra) with those obtained using airborne in situ measurements of h. They also introduced a correction factor (typically 1.06–1.38) to account for this effect. Their findings lead to several conclusions.

[13] First of all, for a correct cloud top height retrieval, one should fully account for a photon transport and multiple scattering inside a cloud. This is confirmed also by a recent study of *Vanbauce et al.* [2003]. Therefore the substitution of a real cloud by a Lambertian reflector model leads to potentially large retrieval errors, depending on an actual cloud geometrical thickness.

[14] Second, the cloud geometrical thickness l can be estimated from independent satellite measurements [*Asano et al.*, 1995; *Kuji and Nakajima*, 2002]. Then retrieved cloud geometrical thickness might be used to obtain a realistic estimation of the light absorption inside a cloud

and therefore to reduce uncertainties in the cloud top altitude measurements. Such a suggestion was made for the first time by *Saiedy et al.* [1965]. Following this path, *Asano et al.* [1995] and *Kuji and Nakajima* [2002] used the oxygen A band for the cloud geometrical thickness determination for several case studies. Note that *Hayasaka et al.* [1995] used the solar reflection at 0.94 μm water vapor absorption band to estimate l.

[15] The development of the radiative transfer theory, an accurate oxygen absorption vertical profiling, and rapid progress in computer technology allowed to solve the problem of cloud top height determination using O_2 A band for a known value of the cloud geometrical thickness (at least for homogeneous cloud layers) [see, e.g., *Fischer and Grassl*, 1991]. For this, one should run the radiative transfer code for underlying surface-cloudy atmosphere system for lines inside the oxygen A band and minimize the difference between measured and simulated oxygen absorption band spectra. The cloud optical thickness, cloud thermodynamic state, and effective radius of particles, which are also needed in fitting procedure, can be obtained from measurements outside gaseous absorption bands as specified, e.g., by *Nakajima and King* [1990] and *Knap et al.* [2002]. In a similar way the cloud geometrical thickness can be estimated (for a known cloud top height, e.g., from space lidar measurements).

[16] The inverse problem can be also posed for a simultaneous determination of cloud top height and cloud geometrical thickness. For this, however, a high spectral resolution and multispectral measurements in the oxygen A band are needed. The alternative is the use of the oxygen B band centered at 687 nm, other molecular absorption bands, or their combinations.

[17] It should be stressed that exact radiative transfer calculations cannot be applied for satellite operational algorithms of the cloud top height determination owing to high requirements in respect to a computational speed. This prompts for a use of a look-up table approach. However, the estimation of the size of such a look-up table gives at least 10^8 cases. The size of the database can be in principle reduced using the polynomial approach [*Fischer and Grassl*, 1991] or neural networks techniques [*Fischer et al.*, 2000].

[18] The main shortcoming of these methods is, however, inflexibility. For instance, the change of the position, width, or the number of spectral channels forces to construct a new database or neural network training. This does not allow to use algorithms developed for a given spectrometer or radiometer to interpret data obtained from different instruments on board multiple satellite platforms using the same database constructed. Similar problems arise also if one needs to feed the algorithm with updated spectroscopic information.

[19] A different approach to reducing the size of the database is based on the use of the asymptotic radiative transfer theory [*van de Hulst*, 1980]. This allows at the same time to preserve a wide range of the model applicability in respect to cloud parameters and illumination/observation geometry. This is similar to numerical methods of the radiative transfer equation solution in this respect. Such a technique is used, e.g., in the MODIS cloud retrievals for the estimation of cloud optical thickness and the droplet/crystal size determination [*King et al.*, 1997] if the cloud optical thickness is larger than 10. Then the accuracy of the asymptotic theory is better than 1%, which is smaller then possible error in a forward model.

[20] We propose to extend this technique of the database reduction to the molecular absorption bands. To this end, modified asymptotic equations [*Kokhanovsky and Rozanov*, 2003, 2004], which have an accuracy typically better than 5% for a cloud optical thickness larger than 5, can be used. The exploration of such a possibility for the problem of the retrieval of cloud geometrical parameters (h, l) is a main task of this paper.

[21] Thinner clouds can be in principle handled by a look-up table approach. However, such cloud systems are highly inhomogeneous in a horizontal direction, making the application of the standard one-dimensional radiative transfer equation not justified. Therefore we consider only the case of optically thick clouds here.

2. Forward Model

2.1. Radiative Transfer Model: The Monochromatic Case

[22] The analytical radiative transfer forward model, which is used here to develop the cloud top height and geometrical thickness retrieval algorithm, is described by *Kokhanovsky and Rozanov* [2003]. They also studied the accuracy of the model, which is typically better than 5% for the calculation of the reflection function at the top of atmosphere (at the cloud optical thickness larger than 5).

[23] For the sake of completeness we formulate the model here as well without any derivations, which can be found elsewhere [*Kokhanovsky and Rozanov*, 2003]. The geometry of the problem is given in Figure 1. Unpolarized solar light illuminates the aerosol-gaseous cloudy atmosphere in the direction $\vec{\Omega}_0$ (ϑ_0, φ_0), and a receiver detects the reflected light intensity I in the direction, specified by $\vec{\Omega}$ (ϑ, φ). Here $\vartheta_0 = \arccos \xi$ and $\vartheta = \arccos |\eta|$ are zenith incident and observation angles, respectively; φ_0 and φ (not shown in Figure 1) are correspondent azimuth angles. We will assume that $\varphi_0 = 0$. Then the azimuth difference between incident and reflected beams directions is given by the angle φ.

[24] A single horizontally homogeneous plane-parallel cloud layer is characterized by a top height h and the geometrical thickness l (see Figure 1). Both h and l can be in principle arbitrary. However, we assume that $l \geq 5\ell$ (or $\tau \geq 5$), where $\ell = \sigma_{ext}^{-1}$ is the photon free path length in a cloud. For a typical value of $\ell = 20$ m, it follows: $l \geq 100$ m. This gives an approximate lower value of the cloud geometrical thickness, which can be handled in the framework of our model. Cloud top height can vary from approximately 0.1 km till the top of atmosphere (TOA) in the model. However, note that terrestrial water and ice clouds, having large optical thickness, do not penetrate to heights larger than approximately 10–15 km, depending on the latitude.

[25] Vertical profiles of the gaseous and aerosol absorption and scattering are fully accounted for in the model as described by *Kokhanovsky and Rozanov* [2003]. We also account for a vertical variation of a cloud single scattering albedo, taking into consideration the increase of gaseous absorption toward the cloud base. The vertical variation of the cloud liquid content is fully accounted for as well.

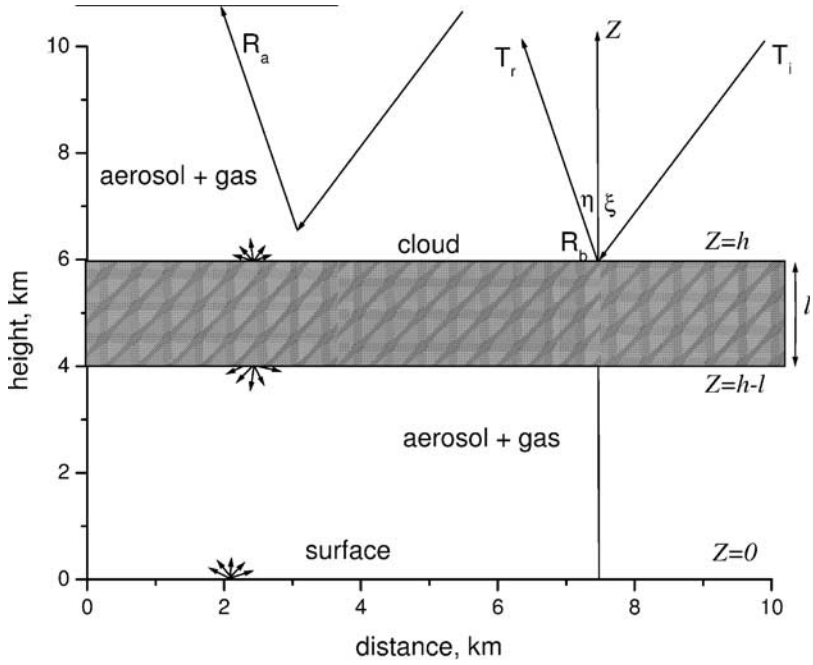

Figure 1. The geometry of the problem.

However, the phase function is assumed to be the same in all parts of a cloud. It is found using the Mie theory [*Kokhanovsky*, 2001] for the effective radius (the ratio of the third to the second moment of the droplet size distribution) equal to 6 μm as in *Deirmendjian*'s [1969] cloud C1 model.

[26] The TOA monochromatic reflection function $R(\lambda, \vartheta_0, \vartheta, \varphi)$ is related to the reflected monochromatic light intensity $I(\lambda, \vartheta_0, \vartheta, \varphi)$ by the following relationship [*Thomas and Stamnes*, 1999]:

$$R(\lambda, \vartheta, \vartheta_0, \varphi) = \frac{I(\lambda, \vartheta, \vartheta_0, \varphi)}{F(\lambda)\cos\vartheta_0}, \tag{1}$$

where $\pi F(\lambda)\cos\vartheta_0$ is the incident spectral solar flux density on the TOA. The value (1) can be easily obtained from measurements performed by various radiometers and spectrometers placed on satellite platforms [*Liou*, 1992].

[27] Following the results given by *Kokhanovsky and Rozanov* [2003], the TOA reflection function R is presented as a sum of two terms (see Figure 1):

$$R = R_a + T_i R_b T_r, \tag{2}$$

where R_a describes light scattering and radiative transfer in the atmosphere above a cloud (with account for both gaseous and particle scattering and absorption). The value of R_b is due to cloud-underlying atmosphere and surface contribution (see Figure 1). The multiplier T_i accounts for the extinction of the direct solar light on the path from the Sun to the cloud top, and T_r accounts for the same effect but on the way from a cloud to a satellite receiver (see Figure 1). We omit arguments in functions in equation (2) for the sake of simplicity.

[28] The scattering of light above clouds is rather weak. Thus the value of R_a is calculated in the single scattering approximation (see Appendix A).

[29] It should be pointed out that coupling between atmospheric layers above and below cloud top is neglected in equation (2). To account partially for this coupling and multiple light scattering above the cloud top, we assume for a product $T = T_i T_r$:

$$T = \exp\left[-\tau'\left(\xi^{-1} + \eta^{-1}\right)\right], \tag{3}$$

where

$$\tau' = \sum_{i=1}^{N} \int_h^H C^G_{abs,i}(z) c_i(z) dz. \tag{4}$$

Here $H = 60$ km is the assumed TOA height, $C^G_{abs,i}(z)$ is the ith gas absorption cross section, N is the total number of gases present, c_i is the ith gas concentration, and $\xi = \cos\vartheta_0$, $\eta = |\cos\vartheta|$. Therefore only extinction owing to gaseous absorption contributes in τ' in the framework of our forward model.

[30] Actually, the value of τ' should include also extinction by aerosol particles (the optical thickness τ^A) and molecules (the optical thickness τ^R). We neglect them in equation (3), which results in increase of T (and $T_i R_b T_r$ in equation (2)). This partially compensates for multiple light scattering in the layer above cloud, which otherwise is completely neglected in this study. Note that this is a standard method for a partial account of multiple light scattering effects in the problems of the atmospheric correction. However, the definition of τ' in equation (3) differs depending on the problem and a spectral range studied [see, e.g., *Gordon et al.*, 1983; *Wrigley et al.*, 1992; *Wang and King*, 1997].

[31] Now we consider the below−cloud top contribution R_b. The general expression for this term for the cloud-underlying Lambertian surface with the albedo A is well known [*Liou*, 1992]. It has the following form, if we neglect

the contribution of the direct light, which is a valid assumption for thick clouds considered here:

$$R_b(\vartheta, \vartheta_0, \varphi) = R_c(\vartheta, \vartheta_0, \varphi) + \frac{A t_c(\vartheta_0) t_c(\vartheta)}{1 - A r_c}, \quad (5)$$

where R_c (ϑ_0, ϑ, φ) is the cloud reflection function at $A = 0$, t_c (ϑ) is the diffused transmittance of a cloud layer, and r_c is the spherical albedo of a cloud. Convenient approximate equations for R_c (ϑ_0, ϑ, φ), t_c (ϑ), and r_c are summarized in Appendix A.

[32] Equations (2), (3), (5), and those given in Appendix A do not completely solve the problem we face. Indeed, there is aerosol-gaseous medium between underlying surface and a cloud base (see Figure 1). It will influence the relationship (5) obtained for the case of a transparent layer between a cloud and a ground surface.

[33] To approximately account for this influence, we substitute A in equation (5) by the effective albedo [*Kokhanovsky and Rozanov*, 2003]

$$A^* = r_a + \frac{A t_a^2}{1 - A r_a}, \quad (6)$$

where r_a is the spherical albedo of the aerosol layer always existing between a cloud and an underlying surface (see Figure 1) and t_a is the aerosol total transmittance. We will neglect the aerosol absorption at this point and assume that $t_a = 1 - r_a$. Thus for the calculation of A^* we should know the value of r_a. Accounting for the fact that the aerosol optical thickness is usually small (smaller than 0.1–0.3) and the aerosol contribution to the TOA reflectance from underneath of thick clouds is weak, we expect that rather coarse approximations for the calculation of r_a can be used. In particular, we have calculated r_a in the framework of the single scattering approximation, described by *Wiscombe and Grams* [1976] (see Appendix A). For thicker aerosol layers the approximation developed by *Kokhanovsky and Mayer* [2003] can be used.

[34] To complete the model, we also account for the light absorption of diffused light fluxes by gases present in a layer between a cloud and an "effective" underlying surface. To do so, we multiply t_c (ϑ_0) and t_c (ϑ) in equation (5) by the flux transmittance [*Feigelson*, 1984; *Li*, 2000]:

$$\gamma = 2 \int_0^1 d\xi \, \xi \exp\left[-\frac{\tau^*}{\xi}\right], \quad (7)$$

where τ^* is the optical thickness due to absorbing gases in a layer between a cloud bottom and a ground surface. Note that it follows with a high accuracy [*Kokhanovsky and Rozanov*, 2003]: $\gamma \approx \exp(-1.7\tau^*)$ at $\tau^* < 0.4$.

[35] Summing up, we have the following final approximate relationship for the TOA reflection function:

$$R(\vartheta, \vartheta_0, \varphi) = R_a(\vartheta, \vartheta_0, \varphi) + \left[R_c(\vartheta, \vartheta_0, \varphi) + \frac{A^* \gamma^2 t_c(\vartheta_0) t_c(\vartheta)}{1 - A^* r_c}\right] T, \quad (8)$$

where A^* is given by equation (6) and approximate analytical formulae for R_a (ϑ, ϑ_0, φ), R_c (ϑ, ϑ_0, φ), r_c, t_c (ϑ_0) are presented in Appendix A. In conclusion, we emphasize that our model accounts for (see Figure 1): (1) light extinction on paths from Sun to a cloud and from a cloud to a satellite; (2) multiple photon scattering inside a cloud; (3) single photon scattering above a cloud; (4) surface and aerosol light reflection and absorption beneath a cloud; and (5) vertical variation of scattering and absorption characteristics of gases and particulate matter both inside and outside of a cloud. Note that some elements of the advanced forward model presented here can be used far beyond a rather narrow topic considered in this paper.

2.2. Radiative Transfer in a Finite Spectral Interval: The Correlated *k* Distribution Scheme

[36] The TOA intensity $I_{\Delta\lambda}$, measured by a radiometer or spectrometer, is in fact an integral of the monochromatic intensity $I(\lambda, \vartheta_0, \vartheta, \varphi)$ taken with respect to the wavelength. It can be presented by the following equation:

$$I_{\Delta\lambda}(\vartheta_0, \vartheta, \varphi) = \int_{\lambda - L}^{\lambda + L} f(\lambda, \lambda') I(\lambda', \vartheta_0, \vartheta, \varphi) d\lambda', \quad (9)$$

where $\Delta\lambda$ is the spectral resolution of the instrument and $f(\lambda, \lambda')$ is the instrument spectral response function, normalized as

$$\int_{\lambda - L}^{\lambda + L} f(\lambda, \lambda') d\lambda' = 1. \quad (10)$$

It is assumed that $f(\lambda, \lambda')$ differs from zero only in the interval $\lambda' \in [\lambda - L, \lambda + L]$, where λ is the central wavelength of the instrument response function. A similar integration should be performed to find the value of $\pi F_{\Delta\lambda} \cos\vartheta_0$ (the incident solar flux density on the TOA in the spectral range $[\lambda - L, \lambda + L]$), which is needed to determine the polychromatic reflection function

$$R_{\Delta\lambda}(\vartheta, \vartheta_0, \varphi) = \frac{I_{\Delta\lambda}(\vartheta, \vartheta_0, \varphi)}{F_{\Delta\lambda} \cos\vartheta_0}. \quad (11)$$

[37] The shape and the half-width of the function $f(\lambda, \lambda')$ is only of a minor importance for measurements outside of atmospheric gaseous absorption bands. This is not the case, of course, for absorption bands of atmospheric gases (e.g., O_2, H_2O, CO_2, N_2O, CH_4, etc.), which have an extremely complicated structure. The response function $f(\lambda, \lambda')$ depends on the particular instrument. For the theoretical study, this function can be taken in the following form:

$$f(\lambda', \lambda) = \begin{cases} 1/\Delta\lambda, & \lambda' \in [\lambda - \Delta\lambda/2, \lambda + \Delta\lambda/2] \\ 0, & \text{in other cases} \end{cases}, \quad (12)$$

which is a simple box function. Then we have $L = \Delta\lambda/2$. Also, one can use the Gaussian function:

$$f(\lambda, \lambda') = \frac{1}{\sqrt{2\pi}\Delta} \exp\left(-\frac{(\lambda - \lambda')^2}{2\Delta^2}\right), \quad (13)$$

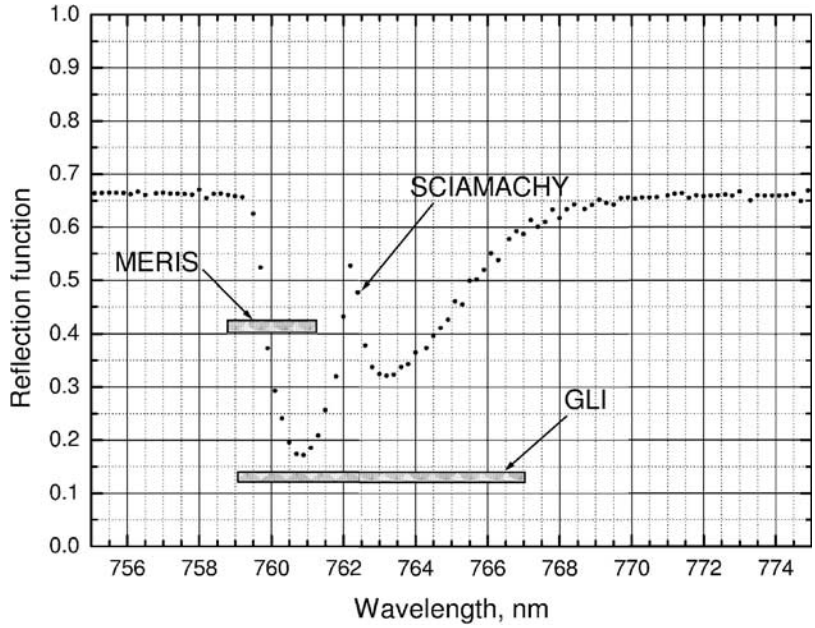

Figure 2. The top-of-atmosphere spectrum measured by SCIAMACHY (points) for a cloudy scene over the Alps on 8 August 2002. Band widths of MERIS and GLI (shaded strips) are also shown. The resolution of GOME (almost the same as in SCIAMACHY) is not shown.

where it is assumed that $L \to \infty$. In practical calculations we will assume that $L = 3\Delta$.

[38] It follows from equation (9) that

$$I_{\Delta\lambda}(\vartheta_0, \vartheta, \varphi) = \sum_{i=1}^{M} \varsigma_i f(\lambda, \lambda_i) I(\lambda_i, \vartheta_0, \vartheta, \varphi), \qquad (14)$$

where ς_i are the quadrature coefficients and λ is the central wavelength. Owing to the oscillating character and the complex structure of the function $I(\lambda)$ in the oxygen band, the number M should be large (typically 1000 at $L = 0.5$ nm). This is impractical, however, because the calculation of $I(\lambda_i, \vartheta_0, \vartheta, \varphi)$ using integrodifferential radiative transfer equation is a complex task, which takes a considerable time.

[39] A so-called correlated k distribution scheme allows to reduce considerably the number of terms in equation (14). This is achieved replacing equation (14) by the following approximate expression:

$$I_{\Delta\lambda}(\vartheta_0, \vartheta, \varphi) = \sum_{j=1}^{m} f(\lambda, \lambda_j) S(\lambda_j, \vartheta_0, \vartheta, \varphi), \qquad (15)$$

where $m \ll M$ and $S(\lambda_j, \vartheta_0, \vartheta, \varphi) = \sum_{\alpha=1}^{5} D_\alpha I_\alpha(\vartheta_0, \vartheta, \varphi)$. The theory behind such a replacement is called the correlated k distribution scheme and described elsewhere [see, e.g., *Lacis and Oinas*, 1991; *Buchwitz*, 2000; *Buchwitz et al.*, 2000]. We have used constants D_α given by *Buchwitz* [2000]. The values of $I_\alpha(\vartheta_0, \vartheta, \varphi)$ are calculated using the monochromatic radiative transfer equation for five precalculated profiles of the molecular oxygen absorption cross section (or exponential sum fitting coefficients [*Buchwitz et al.*, 2000]), depending on the temperature, pressure, and the actual value of λ_j. Values of the oxygen absorption cross section used are given by *Buchwitz* [2000]. The correspondent database has been integrated in the SCIATRAN radiative transfer package [*Rozanov et al.*, 2002] and has been used in this work.

[40] *Buchwitz et al.* [2000] proposed to use values of λ_j distributed from 755 to 775 nm (see Figure 2) with the step $\delta = 0.05$ nm. This allowed to have an error smaller than 2% [*Buchwitz*, 2000] as compared to line-by-line calculations. Clearly we have for the value of m:$m = [\Delta\lambda/\delta]$ for a box function (12). We have approximately for a Gaussian function (13): $m = [6\Delta/\delta]$. Therefore m depends on the spectral resolution of the instrument. Characteristic examples of values $\Delta\lambda$ of selected satellite instruments are presented in Table 1. In particular, we give data for the Global Imager (GLI) [*Nakajima et al.*, 1998], POLDER [*Hagolle et al.*, 1999], the Global Ozone Monitoring Experiment (GOME) imaging spectrometer [*Burrows et al.*, 1999], the Scanning Imaging Absorption Spectrometer for Atmospheric Chartography (SCIAMACHY) [*Bovensmann et al.*, 1999], and the Medium Resolution Imaging Spectrometer (MERIS) [*Bezy et al.*, 2000]. Note that GOME, SCIAMACHY, and MERIS are operating in space at the moment.

[41] Figure 2 shows the spectral resolution of selected spectrometers as related to the oxygen A bandwidth. We see that both GLI and MERIS have much larger bandwidths as compared to SCIAMACHY and GOME instruments. Clearly the actual bandwidth and number of spectral points, where measurements are performed, influences the accuracy of the cloud top height retrieval in a great extent.

[42] Let us substitute equation (8) in equation (15). Then we have for the proposed quasi-analytical model of the radiative transfer in a finite spectral interval:

$$R_{\Delta\lambda}(\vartheta_0, \vartheta, \varphi) = \sum_{j=1}^{m} f(\lambda, \lambda_j) \Re(\lambda_j, \vartheta_0, \vartheta, \varphi), \qquad (16)$$

Table 1. Characteristics of Selected Space Instruments, Related to Measurements of the Backscattered Light in the Oxygen A Band (7550–7750 Å)

Instrument	Platform	Year	Spectral Interval/Wavelength, Å	Spectral Resolution, Å	Spatial Resolution, km^2
GOME	ERS-2	1995	5760–7940	3.3	40 × 320
SCIAMACHY	ENVISAT	2002	6040–8050	4.8	30 × 60
MERIS	ENVISAT	2002	7600	25	0.3 × 0.3 or 1.1 × 1.1
GLI	ADEOS-II	2002	7630	80	1.0 × 1.0
POLDER	ADEOS-II	2002	7633	100	6.0 × 7.0
			7651	400	

where $\Re(\lambda_j, \vartheta_0, \vartheta, \varphi) = \sum_{\alpha=1}^{5} D_\alpha R_\alpha(\vartheta_0, \vartheta, \varphi)$. The values of $R_\alpha(\vartheta_0, \vartheta, \varphi)$ are calculated at given effective absorption cross sections as discussed by *Buchwitz et al.* [2000].

[43] The crucial point in calculations according to equation (16) is an account for the vertical distribution of the oxygen concentration (see, e.g., equation (4)). Also, one should account for the variation of the oxygen effective absorption cross section $C_{abs,\alpha j}$ with temperature and pressure. This is done using the database of $C_{abs,\alpha j}$, calculated by M. Buchwitz (personal communication, 2003) for the values of λ_j in equation (15) using the HITRAN_2000 database [*Rothman et al.*, 2003].

[44] The accuracy of equation (16) was studied by *Kokhanovsky and Rozanov* [2003] for a realistic vertically inhomogeneous atmosphere. One example of the performance of this equation is shown in Figure 3 for the GOME resolution with the instrument response function according to equation (13). We see that errors for the case considered are very low even inside the minimum of the absorption band, where the main assumption behind the derivation of the result for R_c in equation (8) (namely weak light absorption) [see, e.g., *Kokhanovsky et al.*, 2003] is violated. This is due to a comparatively large contribution of the term R_a (small values of T) in this case.

3. Inverse Problem

3.1. One-Parameter Retrieval Algorithm

[45] Let us consider the inverse problem using equations introduced above. We assume at first that all parameters of our problem except the cloud top height h are known. Then the value of h can be found from spectral measurements in the oxygen A band using the following semianalytical technique.

[46] Fist of all, we present equation (16) in the form of a Taylor expansion:

$$R = R(h_0) + \sum_{l=1}^{\infty} a_l (h - h_0)^l, \tag{17}$$

where $a_l = R^{(l)}(h_0)/l!$, and we have omitted for the sake of simplicity the index $\Delta\lambda$ and angular variables (see equation (16)). Here $R^{(l)}(h_0)$ is the l derivative of R at the point h_0. The next step is the linearization, which is a

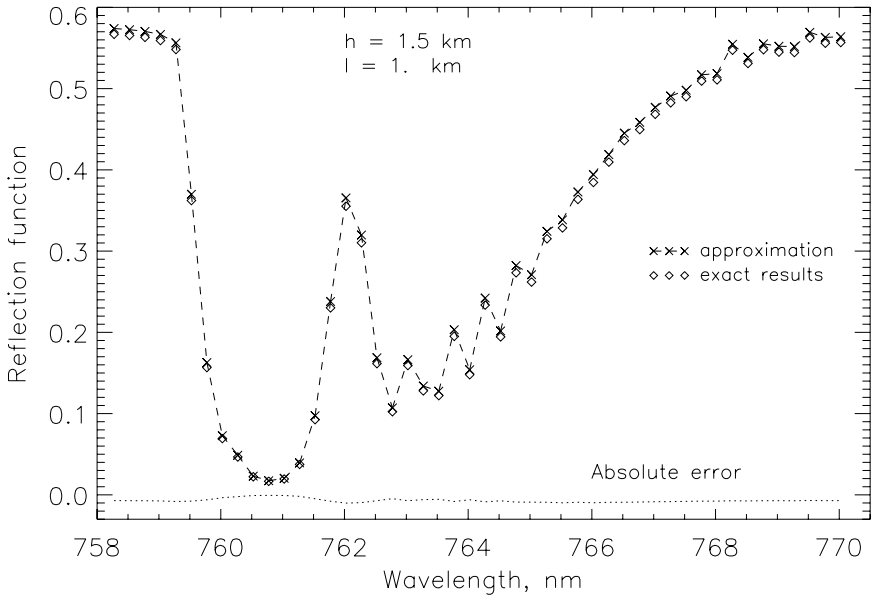

Figure 3. The spectral reflection function of a cloudy medium in the oxygen A band calculated using equation (16) and the exact radiative transfer code at the cloud optical thickness equal to 20 and solar angle equal to 60° and nadir observation for the cloud C1 model [*Deirmendjian*, 1969] and the same aerosol and gaseous profiles as those specified by *Kokhanovsky and Rozanov* [2003]. Calculations correspond to the GOME resolution. The black underlying surface is assumed.

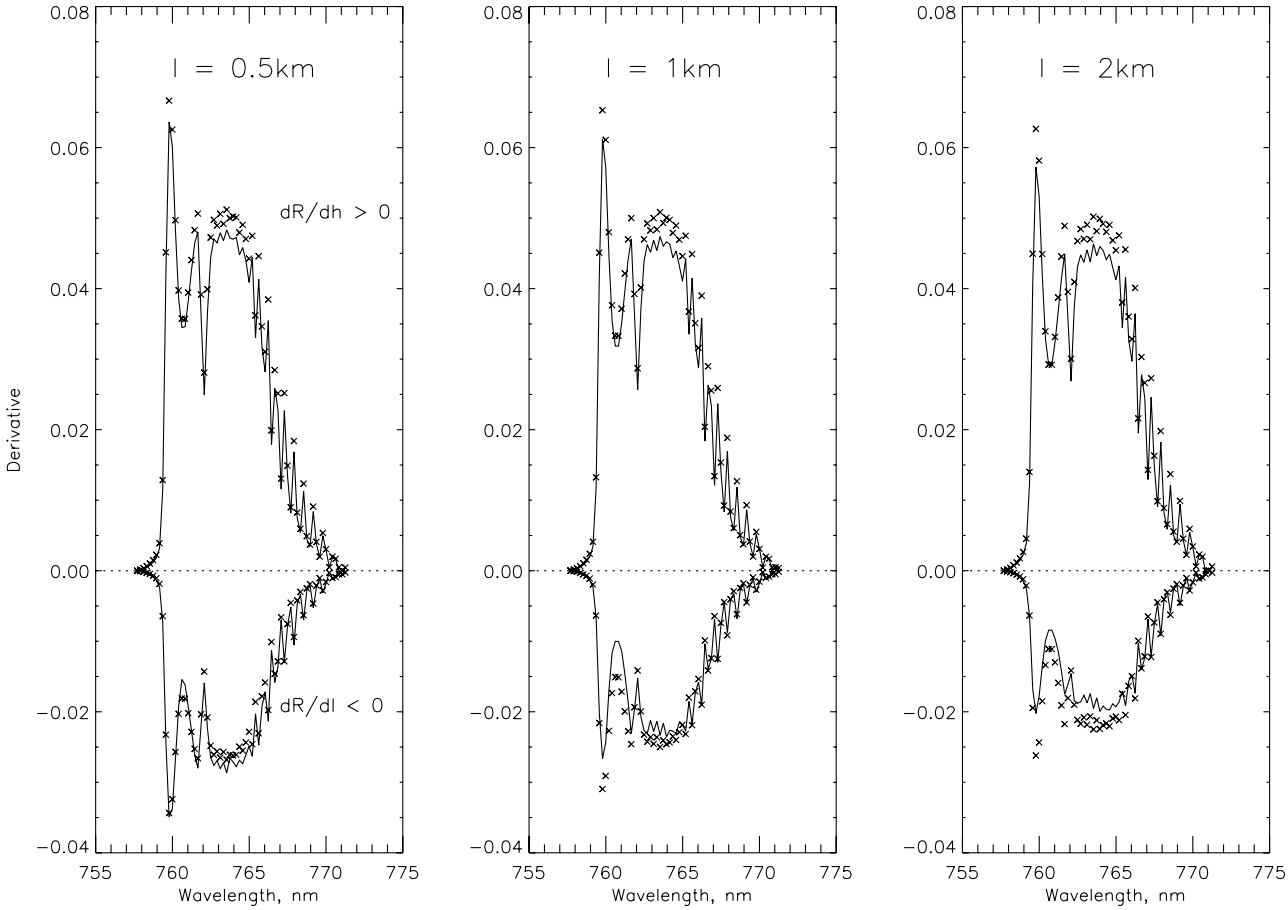

Figure 4. The spectral dependence of derivatives $\frac{dR}{dh}$ and $\frac{dR}{dl}$ calculated using exact radiative transfer code (crosses) and our approximation (lines) for the same conditions as in Figure 3 except the solar angle equal to 53 degrees and cloud top height equal to 3 km for l = 0.5, 1, and 2 km.

standard technique in the inversion procedures [*Rozanov et al.*, 1998; *Rodgers*, 2000]. We found that the function $R(h)$ is close to a linear one in a broad interval of the argument change [*Kokhanovsky and Rozanov*, 2003]. Therefore we neglect nonlinear terms in equation (17). Then it follows:

$$R = R(h_0) + R'(h_0)(h - h_0), \tag{18}$$

where $R' = \frac{dR}{dh}$. We assume that R is measured at several wavelengths in the oxygen A band. Then instead of the scalar quantity R, we can introduce the vector $\vec{R}_{mes}$ with components ($R(\lambda_1)$, $R(\lambda_2)$, ... $R(\lambda_n)$). The same applies to other scalars in equation (17).

[47] Therefore equation (18) can be written in the following vector form:

$$\vec{y} = \vec{a}x, \tag{19}$$

where $\vec{y} = \vec{R}_{mes} - \vec{R}(h_0)$, $\vec{a} = \vec{R}'(h_0)$ and $x = h - h_0$. Note that both measurement and model errors are contained in equation (19). The solution $\hat{x}$ of the inverse problem is obtained by the minimizing the following cost function [*Rodgers*, 2000]:

$$\Phi = \|\vec{y} - \vec{a}x\|^2, \tag{20}$$

where $\| \ \|$ means the norm in the Euclid space of the correspondent dimension. It follows from equation (20) [*Rodgers*, 2000] that

$$\hat{x} = \frac{(\vec{a}, \vec{y})}{(\vec{a}, \vec{a})}, \tag{21}$$

where $(\vec{a}, \vec{y})$ means the scalar product and $\hat{x}$ gives the value of x, where the form (20) takes a minimum. Therefore, knowing values of the measured spectral reflection function R_{mes} and also values of the calculated reflection function R and its derivative R' at $h = h_0$ and several wavelengths, the value of the cloud top height can be found from equation (21) and equality: $h = \hat{x} + h_0$. The value of h_0 can be taken equal to 1.0 km, which is a typical value for low level clouds. The main assumption in our derivation that the dependence of R on h can be presented by a linear function on the interval x [*Kokhanovsky and Rozanov*, 2003]. Note that the same equations can be used for the cloud geometrical thickness determination (with the substitution of h by l, see equation above).

[48] Above, either value of h (or l) is assumed to be unknown. Our algorithm, however, has also a capability to find these two parameters (and also some other auxiliary information) simultaneously. This requires the minimization

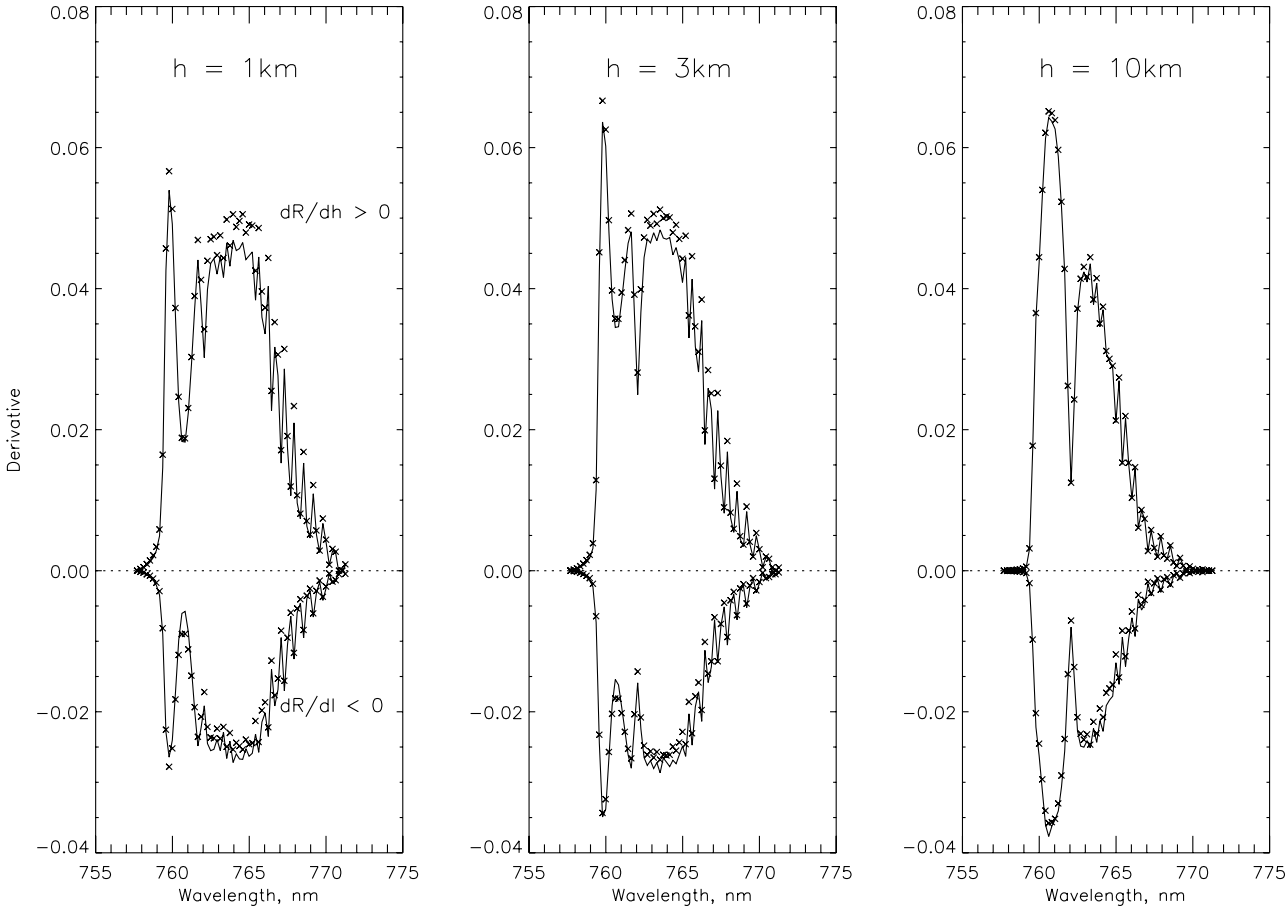

Figure 5. The spectral dependence of derivatives $\frac{dR}{dh}$ and $\frac{dR}{dl}$ calculated using exact radiative transfer code (crosses) and our approximation (lines) for the same conditions as in Figure 4 except the cloud geometrical thickness is equal to 0.5 km and h = 1, 3, 10 km.

of the modified cost function (see equation (20)): $\Phi = \|\vec{y} - \hat{A}\vec{X}\|^2$. The elements of the matrix $\hat{A}$ are correspondent weighting functions [*Rodgers*, 2000]. The solution of the inverse problem is given by the vector parameter $\vec{X}$. The first two components of this vector give corrections to the initially assumed cloud top height and cloud top geometrical thickness. Others include information on auxiliary parameters like the correction due to the assumed half-width of the spectrometer spectral response function.

[49] Values of R and R' are usually found from the numerical solution of the integrodifferential radiative transfer equation for a model atmosphere. They also can be calculated using equation (16). The last possibility allows to speed up the numerical solution of the inversion problem and will be used throughout the paper.

[50] Note that it is possible to calculate derivatives R' analytically. Correspondent expressions for R' are cumbersome. They are not shown here. However, they were derived and used in the retrieval procedure.

[51] We compare numerically obtained from the exact radiative transfer code SCIATRAN [*Rozanov et al.*, 2002] and approximate derivatives in Figures 4 and 5 It follows that derivatives (both with respect to h and l) differ from zero in the oxygen band. This actually allows for the values of h and l determination from the TOA reflectance measurements. It follows that analytical derivatives have a high accuracy. Their calculation is much faster as compared with the numerical perturbation technique, so we prefer their use in the retrieval procedure.

[52] Note that $R'_h = \frac{dR}{dh}$ is positive and $R'_l = \frac{dR}{dl}$ is negative. It confirms that the increase in the cloud top height leads to the increase of the reflectance at the fixed cloud geometrical thickness. The opposite is true for the increase of the cloud geometrical thickness at the fixed cloud top height.

[53] An important step in every inverse problem is to understand the sensitivity of the model to the various possible errors [*Rodgers*, 2000]. They were studied in great detail by several authors using the exact radiative transfer theory [see, e.g., *Wu*, 1985; *Fischer and Grassl*, 1991; *Fischer et al.*, 1991; *O'Brien and Mitchell*, 1992], so we do not repeat these studies here. In particular, *Fischer et al.* [1991] showed that all errors totaled up in the possible error in the cloud top height determination equal to 150 m as compared to in situ cloud top height measurements. The averaging procedure allowed then to reduce the error over the flight distance 20 km down to 40 m [*Fisher et al.*, 1991].

[54] Clearly, if we use synthetic data obtained from the exact radiative transfer theory and also exact calculations for finding R and R', then the error of finding h from equation (21) is close to zero. It is interesting to study how

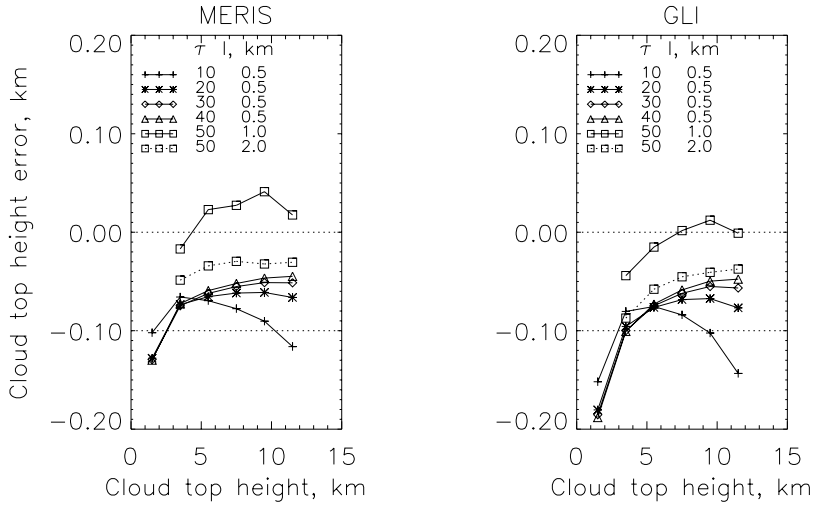

Figure 6. The cloud top height error as the function of the actual cloud top height, obtained from the use of the analytical model presented here for known values of the cloud optical and geometrical thickness. Results for resolutions correspondent to MERIS and GLI instruments are shown (see text). The measured reflection function was simulated using the radiative transfer code SCIATRAN [*Rozanov et al.*, 2002] at the solar zenith angle equal to 60 degrees and nadir observations.

large the error of the cloud top height determination is if we model measured data by the exact theory but retrieve the value of h, using approximate solutions for the reflection function and its derivatives introduced above. This shows us how errors of our forward model transform, e.g., in the error of the cloud top height determination $\Delta = h - h_r$, where h_r is the retrieved value of the cloud top height.

[55] The dependence of Δ on the cloud top height for different values of l, τ is given in Figure 6. The spectral resolutions chosen are correspondent to MERIS and GLI instruments (see Table 1). Note that for these instruments only a single-wavelength measurement in the oxygen A band is performed (see Figure 2). Then we have instead of equation (21):

$$h_r = h_0 + \frac{R_{mes} - R(h_0)}{R'(h_0)}, \tag{22}$$

where h_r gives the retrieved value of the cloud top height. We use instead of measured value of the reflection function R_{mes} in equation (22), the correspondent function, which is obtained from the exact SCIATRAN [*Rozanov et al.*, 2002] radiative transfer calculations. The measurement errors are neglected in this case.

[56] Note that for all retrievals performed in this paper, we have actually used values of R_{mes}, R, and R' normalized to the average value of these functions outside the band (in the interval 755–757 nm (see Figure 3)). This enhances the accuracy of the retrieval.

[57] It follows from Figure 6 that errors Δ of our technique for both instruments are smaller than 200 m, which is much better than the accuracy and which can be obtained from infrared passive techniques. Results for MERIS are slightly better because our approximation works better for smaller absorption [*Kokhanovsky et al.*, 2003], which is the case for the MERIS measurements (see Figure 2). Note that for most of cases the value of Δ is negative, which means that the value of h is overestimated by the our approximate radiative transfer method. Therefore too high values of h are retrieved.

[58] Figure 7 gives the retrieved value of the cloud top height error Δ for different solar zenith angles. We see that the error is not influenced by the illumination condition dramatically. However, generally the error increases with the solar zenith angle. The influence of the solar zenith angle is more important for low clouds, where our technique gives larger retrieval errors.

[59] Although the error of the asymptotic algorithm (up to 200 m) may appear unacceptably large (especially if other possible error sources are accounted for), it is small in comparison with common errors of passive methods used today for the cloud top height determination [*Naud et al.*, 2002]. They typically give the accuracy not better than 1km in the value of h [*Naud et al.*, 2002].

[60] The question arises if the error of the retrieval can be reduced if the exact theory is applied to finding the cloud altitude from measurements performed in terrestrial atmosphere. As we stated above, the error Δ for synthetic data will be close to zero in this case. However, we believe that our analytical asymptotic cloud retrieval algorithm should give errors of h close to that obtained if the exact theory is applied to the interpretation of the experimental data obtained from measurements in the terrestrial atmosphere. This is mostly due to the fact that here plays a major role not the difference (approximately 5% or even less; see Figure 3) between the exact and asymptotic theory, but the uncertainty related to the forward model, which is basically the same both for the exact theory and approximation and does not necessarily correspond to the case presented during measurements (e.g., cloud horizontal inhomogeneity and the existence of several cloud layers).

[61] However, this question can be cleared out only after such experiments are performed in situ, which is a complex task. We hope to make such a study in future. For this, collocated airborne and satellite measurements over extended cloud fields are clearly needed. As it was stated above, the

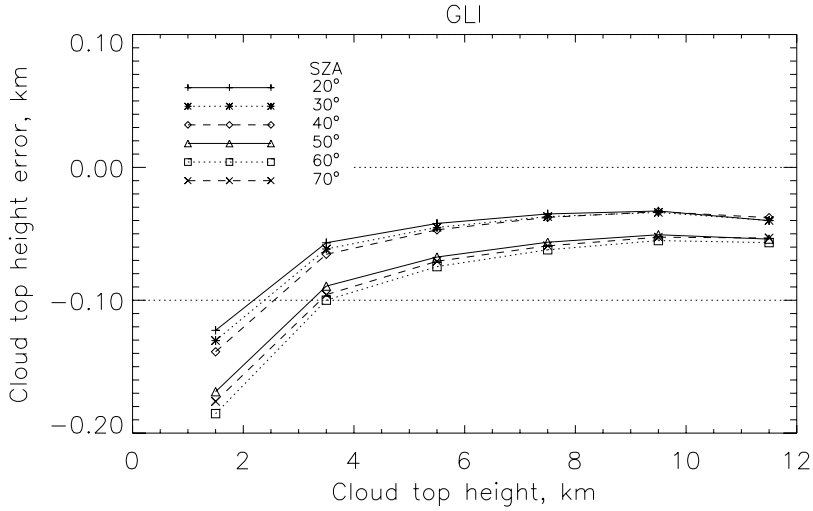

Figure 7. The same as in Figure 6 but for various solar zenith angles (SZA) at $l = 0.5$ km and $\tau = 30$.

exact radiative transfer theory cannot be applied to operational retrievals owing to speed requirements.

[62] Some estimates of errors in the parameter h determination for vertically inhomogeneous and realistic two-layered cloud systems are given in section 4. To make them, we have performed a number of numerical experiments. We emphasize once more that the same algorithm as described above (after a slight modification (change h to l)) can be also used for the cloud geometrical thickness determination (e.g., if h is known from space lidar measurements).

3.2. Two-Parameter Retrieval Algorithm

[63] Generally, both MERIS and GLI (see Table 1) do not allow to find both parameters (h and l) from measurements in the oxygen A band only (one measurement). However, it is possible to obtain the cloud top height from the GLI infrared measurements [*Nakajima et al.*, 1998; *Nakajima*, 2001]. Then this information can be applied (at least in principle) to the determination of the cloud geometrical thickness using the measurement in oxygen A band [*Kuji and Nakajima*, 2002]. However, a possible large error [*Naud et al.*, 2002] in h can influence the results of the cloud geometrical thickness determination in a great extent. To illustrate this, we plot the ratio of derivatives R'_h to R'_l (or $\Upsilon = R'_h/R'_l$) in Figure 8. The parameter Υ gives the relationship of the error in the determination of the cloud geometrical thickness Δl and the error in the cloud top height Δh. Namely, we have: $\Delta l = -\Upsilon \Delta h$.

[64] We see that the error of the cloud geometrical thickness determination is 1.5–3.0 times larger than the error with which the cloud top height is known ($\Upsilon \in [-3.0, -1.5]$; see Figure 8). It means that if the cloud top height is obtained with the accuracy, e.g., 1.0 km, then the cloud geometrical thickness cannot be obtained with the accuracy better than 1.5–3.5 km, which is clearly too large for most of applications. This emphasizes the problems that can be accounted, e.g., in the interpretation of the GLI data with

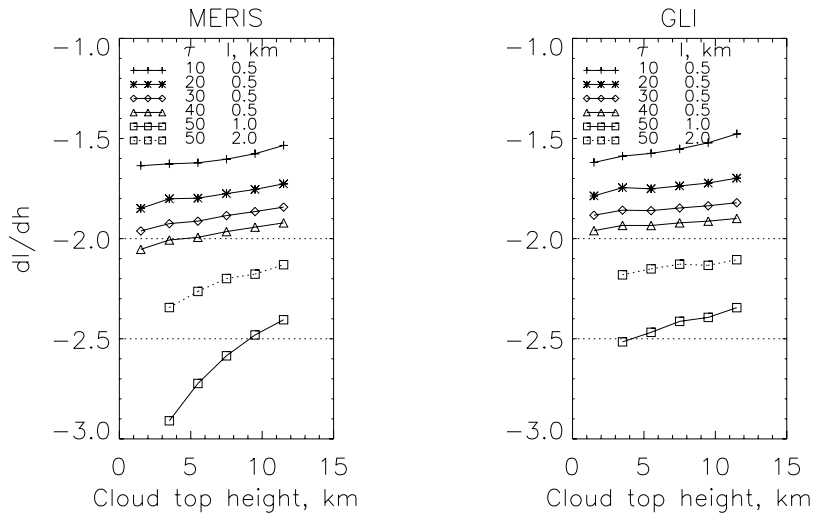

Figure 8. The dependence of derivatives $\frac{dl}{dh} \equiv \frac{R'_h}{R'_l}$ on the cloud top height at the solar zenith angle 60 degrees and the nadir observation for various values of l and τ. Results for resolutions correspondent to MERIS and GLI instruments are shown (see text).

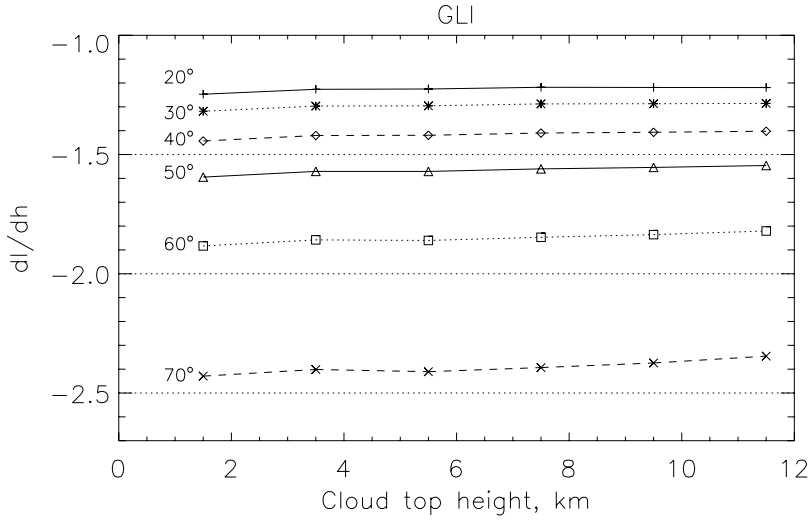

Figure 9. The same as in Figure 8 but for various solar angles at l = 0.5 km and τ = 30.

respect to the cloud top height determination [*Nakajima et al.*, 1998].

[65] Note that the cloud geometrical thickness can be easily obtained from the reflectance measurements in the oxygen A band if the value of cloud top height is known with a high precision (e.g., from space lidar measurements [*Poole et al.*, 2003]).

[66] The dependence of the derivative dl/dh on the solar angle is given in Figure 9. It shows that the high Sun cases are preferable for the remote sensing of the cloud geometrical thickness (for only approximately known value of the cloud top height).

[67] The problem of the determination of both parameters can be partially solved if one uses the neural network approach and trains the inverse algorithm for typical cloudy conditions [*Fischer et al.*, 2000]. However, this also can lead to large retrieval errors if these conditions are not met for a given experiment. The main problem here is a low spectral resolution both GLI and MERIS (see Figure 2), which makes the solution of the problem highly difficult.

[68] This once more emphasizes that a simple Lambertian reflector model cannot be applied for accurate cloud top height retrievals. The value of l is an important parameter, which cannot be neglected.

[69] The difficulty, however, can be avoided, if one uses the measurements from GOME or SCIAMACHY, which have much higher spectral resolution that those of GLI and MERIS (see Table 1). These advanced instruments are also characterized by a larger number of spectral points measured in different regions of the oxygen A absorption band. The shortcomings of GOME or SCIAMACHY as far as cloud research is concerned are related to their large footprints. Therefore instruments with high spatial resolution and also with high spectral resolution in the oxygen A band can improve substantially our knowledge of the terrestrial cloudiness. Note that such an instrument (the Orbiting Carbon Observatory (OCO)) has already been designed [*Kuang et al.*, 2002]. The OCO should be launched in 2007.

[70] Clearly the results presented above can be obtained also for GOME and SCIAMACHY by a special choice of channels for the retrieval (correspondent to channels of GLI or MERIS, see Figure 2). There is even possibility of the optimization of channels for the retrieval to account for the spectral behavior of the error of our model. Note that the error of the retrieval of h for a known l for GOME or SCIAMACHY instrument using measurements for all wavelengths in the oxygen A band is close to data given for GLI. This is because in both cases almost all band is used. In principle, the error can be optimized with respect to the wavelength selection. We do not consider this possibility here, however.

[71] The superiority of GOME and SCIAMACHY instruments is due to the possibility to infer accurately both parameters (h, l) from measurements in the oxygen A band. This is because instead of 1 measurement point in the O_2 A band, we have approximately 66 (for GOME) and 44 (for SCIAMACHY) spectral points (see above).

[72] There are several possibilities for the development of the retrieval algorithm in this case. We chose here the simplest one, which is based on the technique, described in the previous section. Namely, we assume a small geometrical thickness of the cloud equal, e.g., to 100 m and perform the retrieval to find the value of the cloud top height h as described in section 3.1 using all spectral points available. Then the value of the maximal difference δ_f between the calculated O_2 A band spectrum and measured spectrum is derived, taking into account all spectral points. The value of l is increased and the procedure is repeated till the minimum of the function $\delta_f(l)$ is found.

[73] Therefore the solution of the two-parameter problem is reduced to the sequence of solutions of the one-parameter problem of the finding h at given value of l_k (k = 1, ... N) (see section 3.1). Namely it follows that

$$h^{(n)}(l_k) = h^{(n-1)}(l_k) + \frac{\left(\vec{a}\left(h^{(n-1)}, l_k\right), \vec{y}\left(h^{(n-1)}, l_k\right)\right)}{\left(\vec{a}\left(h^{(n-1)}, l_k\right), \vec{a}\left(h^{(n-1)}, l_k\right)\right)}. \qquad (23)$$

The iteration process used to find h (l_k) allows to reduce the influence of the linearization errors [*Rodgers*, 2000] in the case when the initial approximation $h^{(0)}$ (l_k) is far away from the solution of the problem. Note that the process of

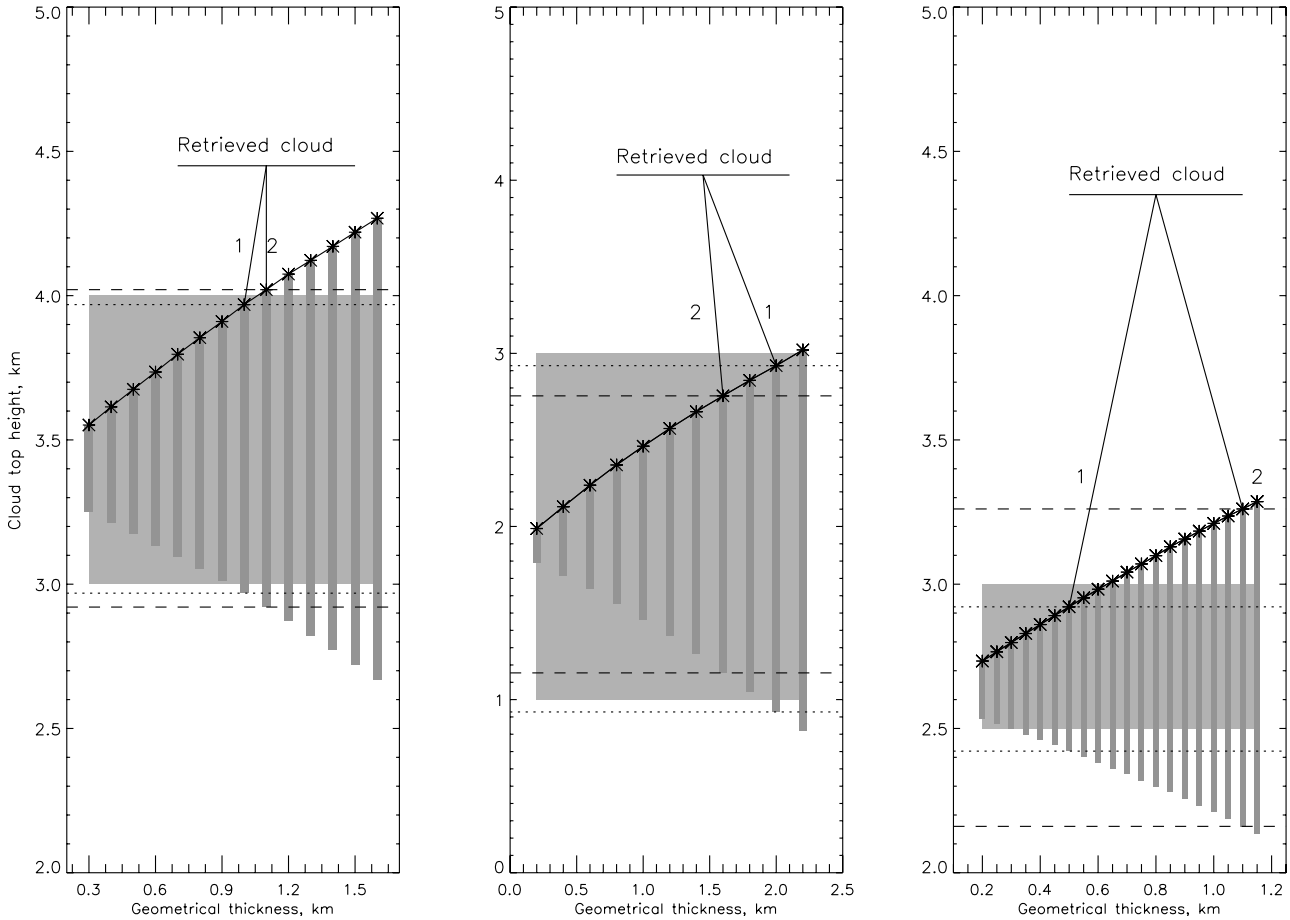

Figure 10. The illustration of the performance of simultaneous cloud top height and cloud geometrical thickness semianalytical retrieval algorithm. Measurements were simulated using SCIATRAN [*Rozanov et al.*, 2002]. The random error of 0.3% was added to measurements. Shaded areas show cloud parameters for a simulated case ("true clouds"). Dashed lines show retrieved clouds. The number 1 is related to the retrieval of cloud top height for a known value of l. The number 2 is related to the case, when both h and l are not known. Calculations are given for the GOME resolution at $\tau = 30$ and nadir observation. The solar zenith angle is equal to 53 degrees. Different panels correspond to different "true clouds" positions.

iterations is terminated when the difference between retrieved values of cloud top heights becomes smaller than 50 m. Then we calculate the value of the error:

$$\delta_f(l_k) = \left\| \vec{y}\left(h^{(n)}, l_k\right) - \vec{a}\left(h^{(n)}, l_k\right) x^{(n)} \right\|^2 \qquad (24)$$

for a spectral range studied.

[74] We emphasize that the algorithm described was developed to demonstrate the dependence of the retrieved cloud top height on the cloud geometrical thickness. Other possible solutions of the inverse problem can be used [*Rodgers*, 2000].

[75] Let us consider now Figure 10, where we assumed a random error of 0.3% for simulated radiances. Note that these radiances are also in error (typically below 5%) owing to our model inaccuracy as compared to SCIATRAN data. The vector $\vec{R}$ is given by a column of numbers for the GOME as specified above.

[76] Note that the case 1 in Figure 10 gives the retrieved cloud top height if the value of l is exactly known. The case 2 corresponds to the case when both h and l are not known and the pair (h, l) is chosen using the location of the minimum of the function $\delta_f(l)$.

[77] Data given in Figure 10 allow to make the following conclusions:

[78] 1. The iteration algorithm (see equation (23)) finds the cloud top height h with the accuracy better than 100 m if the cloud geometrical thickness l is known.

[79] 2. The error of the cloud top height determination increases up to 250 m if both h and l are unknown parameters of the problem. The error of the cloud geometrical thickness is in the range 200–600 m, depending on a particular case studied. Note that the influence of random errors is very profound in this case (even for their small values). This is because this error displaces the minimum of the function $\delta_f(l_k)$ considerably (see equation (24)).

[80] 3. The dependence of the retrieved value of h on l can be approximated by a linear function. Our estimations lead to values of dl/dh in the range 1.6–1.7. This is in an accordance with results shown in Figures 8 and 9.

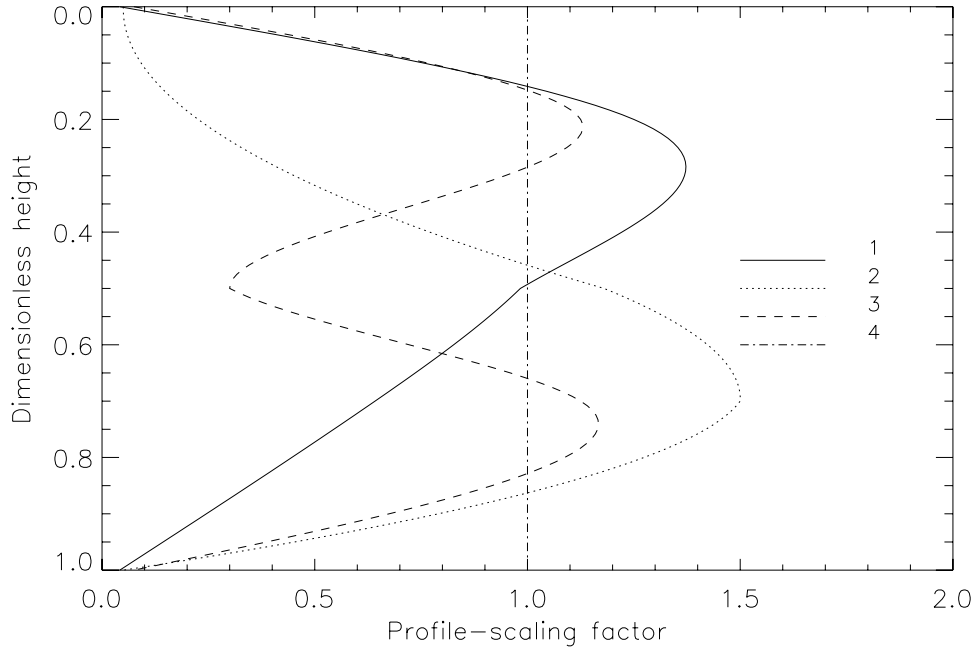

Figure 11. The dependence of the profile-scaling factor on the dimensionless height for four types of LWC profiles (see text for explanation).

[81] Summing up, we see that the retrieval accuracy is quite high if synthetic data are used. In particular, the value of h is found with an accuracy better than 250 m if both h and l are unknown parameters of the problem. The important question is the performance of the algorithm for the case of satellite measurements. Those are considered in a separate publication [*Rozanov et al.*, 2004].

4. Errors of Retrievals as Applied to Vertically Inhomogeneous and Multilayered Clouds

[82] The previous section was devoted to the determination of the parameters h, l, assuming that a cloud field under study can be represented by a single homogeneous layer. Such an assumption is never valid. The concentration and size of droplets in clouds change with height [*Feigelson*, 1984]. Also, multilayered cloud systems are more common than a simple case of a single cloud layer [*Grechko et al.*, 1973, 1975; *Platnick et al.*, 2003]. Many clouds contain also ice crystals of various shapes and not only spherical water droplets. This certainly leads to biases of retrieved parameters if a single liquid water cloud with the constant liquid water content (LWC) is assumed in the retrieval procedure. A brief study of these biases using several numerical experiments is given in this section.

4.1. Influence of the Vertical Profile of the Liquid Water Content

[83] We choose four liquid water content profiles for the study of the influence of these profiles on the retrieval procedure. They are given in Figure 11. The dimensionless height is defined as $\upsilon = (h - z)/(h - b)$, where z is the vertical coordinate, changing from $z = b$ at the cloud bottom to $z = h$ at the cloud top. The profile scaling factor s (υ) (see Figure 11) determines the cloud optical thickness τ and liquid water path W with following equations:

$$\tau = \langle \sigma_{ext} \rangle \int_b^h s(z)dz, \tag{25}$$

$$W = \langle LWC \rangle \int_b^h s(z)dz, \tag{26}$$

where $\langle \sigma_{ext} \rangle$ and $\langle LWC \rangle$ are the average values of the extinction coefficient and LWC inside the cloud. Therefore the liquid water profile inside the cloud is determined as the product s (z) $\langle LWC \rangle$.

[84] The profile of the type 1 (see Figure 11) is found in most of cloud layers [*Feigelson*, 1984]. It gives maximum of the LWC near the top of the cloud. The profile of the second type has been used in calculations of the influence of clouds on climate [*Marchuk et al.*, 1986]. The profile of the third type is the superposition of profiles 1 and 2. The profile 4 corresponds to the vertically homogeneous layer used above. Note that we neglect the possible variability of cloud droplets sizes with height here. Also, it is assumed that ice crystals are absent.

[85] Let us consider now the results of the retrieval of parameters h and l with our algorithm, assuming different types of liquid water content profiles for synthetic data. The inverse algorithm, however, is the same as for the case of the LWC = const. It means that we consider the case when the forward model does not match the realistic cloud system.

[86] For this, we have created synthetic top of atmosphere reflectance data R_{mes} using SCIATRAN [*Rozanov*

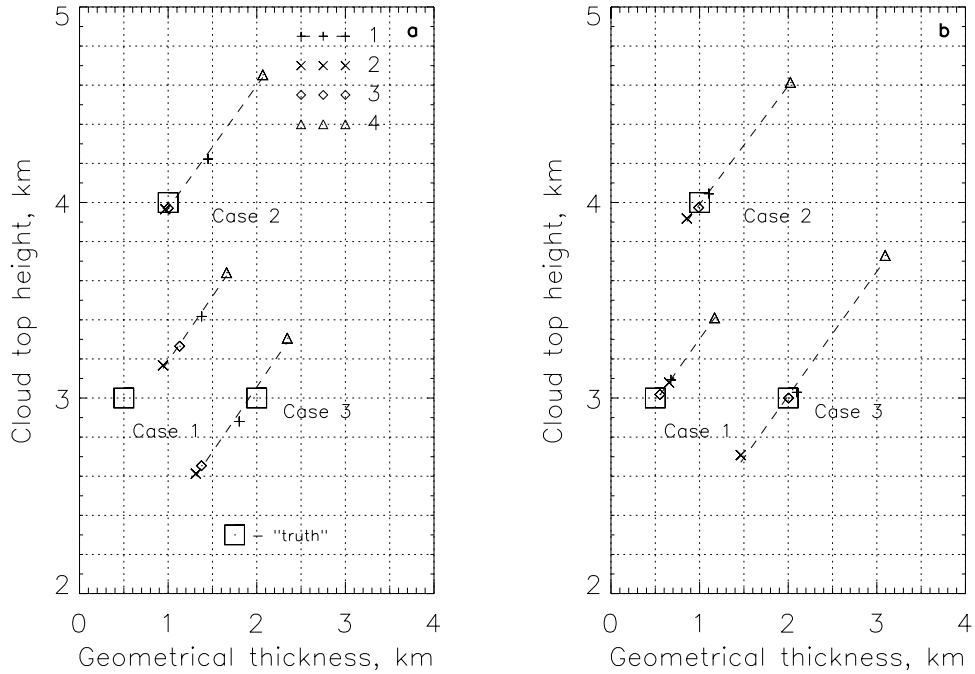

Figure 12. (a) The influence of the vertical profile of the liquid water content (see Figure 11) on the accuracy of the determination of values h, l. The spectral resolution corresponds to GOME. It is assumed that cloud optical thickness is equal to 30 and the solar zenith angle is 53 degrees. The random error is equal to 0.3%. The observation is in the nadir direction. Big squares give the position of the "true" cloud in the coordinates (h, l). Different symbols give results of the retrieval under different choice of the LWC in a cloud (see Figure 11). Numbers in Figure 12a correspond to numbers in Figure 11. The cases 1, 2, and 3 correspond to clouds with values of (h, l) equal to (3.0, 0.5), (4.0, 1.0), and (3.0, 2.0) km, respectively. (b) Same as in Figure 12a, but the synthetic data have been calculated using the semianalytical technique described above (and not SCIATRAN as in Figure 12a).

et al., 2002] for the vertical profile of the type 1. The retrieval results using the synthetic spectra are summarized in Figure 12 for three cases, having the parameters (h, l) equal to (3.0, 0.5) (case 1), (4.0, 1.0) (case 2), and (3.0, 2.0) (case 3). The random error $\varepsilon = 0.3\%$ is added to R_{mes}. It follows from Figure 12a that the error of the cloud top height determination increases up to 600 m if it is assumed that LWC = const. The difference of Figure 12b from Figure 12a is that the value of R_{mes} was calculated not using the SCIATRAN but the asymptotic theory given above. This allows to model the influence of the random error and a wrong LWC profile on results of retrievals. The errors of the radiative transfer model are excluded in this case.

[87] It follows that the influence of the LWC profile is more important for clouds having larger geometrical thickness. For instance, the use of the condition LWC = const in the inversion procedure gives the error of 400 m for the case 1 (l = 0.5 km). The error is equal to 750 m for the case 3 (l = 2 km). The comparison of Figures 12a and 12b shows that the use of the semianalytical cloud retrieval scheme does not lead to the considerable increase of the retrieval error.

[88] Summing up, the use of the assumption LWC = const in the retrieval procedure for the case of realistic vertically inhomogeneous clouds can lead to potentially large errors (up to 600–800m in h and up to 1 km in l). Clearly the assumption of a typical LWC profile (and not LWC = const) in the retrieval procedure for a single cloud case will lead to the decrease of errors mentioned above.

4.2. Influence of the Second Cloud Layer

[89] Let us consider now the case of two-layered cloud systems and their influence on the retrieval procedure on the basis of the assumption of a homogeneous single cloud layer. Generally, the presence of multilayered cloud systems [*Grechko et al.*, 1973, 1975] leads to a great variety of different situations, which differ not only by the number, position, geometrical and optical thickness of cloud layers, but also by a possibility to have water droplets or exclusively ice crystals in different cloud layers.

[90] Let us consider now the results of the retrieval of parameters h and l with our algorithm, assuming different types of two-layered cloud systems. Namely, we will consider the case of two liquid water cloud layers and separately the case of an ice cloud above liquid one. Such situation is a typical one for terrestrial atmosphere.

[91] We start from the case of liquid clouds. For this, we have created synthetic top of atmosphere reflectance data R_{mes} using SCIATRAN [*Rozanov et al.*, 2002] for the two-layered liquid cloud system. Also, we have assumed that the vertical profile of the LWC in both clouds correspond to the type 1, given in Figure 11. The results of retrievals assuming the single-layer cloud system with LWC = const are given in Figures 13 and 14 for various values of optical thickness of upper and lower cloud. The analysis of data

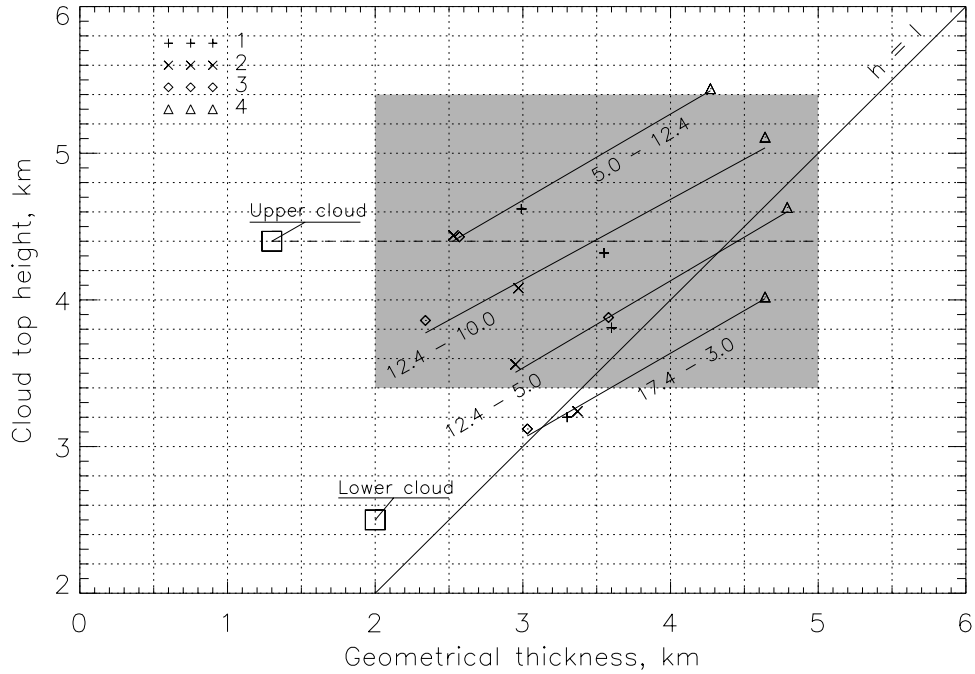

Figure 13. The results of the retrieval of h and l of the cloud system composed of two water cloud layers. The distance between layers $\mathbb{Z}$ is equal to 600 m. Big squares give the position of the "true" cloud in the coordinates (h, l). Different symbols give results of the retrieval under different choices of the LWC in a cloud (see Figure 11). Numbers under curves give the cloud optical thickness of the lower and upper cloud layer, respectively. The solid line ($h = 1$) gives the position of the cloud having the value of h equal to that of l. Dark area corresponds to the upper boundary of the upper cloud ±1 km.

given in these figures, which differ only by the distance $\mathbb{Z}$ between two cloud systems (Z = 600 m for Figure 13 and $\mathbb{Z}$ = 2 km for Figure 14), allows us to reach following conclusions:

[92] 1. The assumption LWC = const and a single cloud layer in the retrieval procedure gives the cloud top height of the vertically inhomogeneous two-layered cloud system with the accuracy equal to ∼1 km.

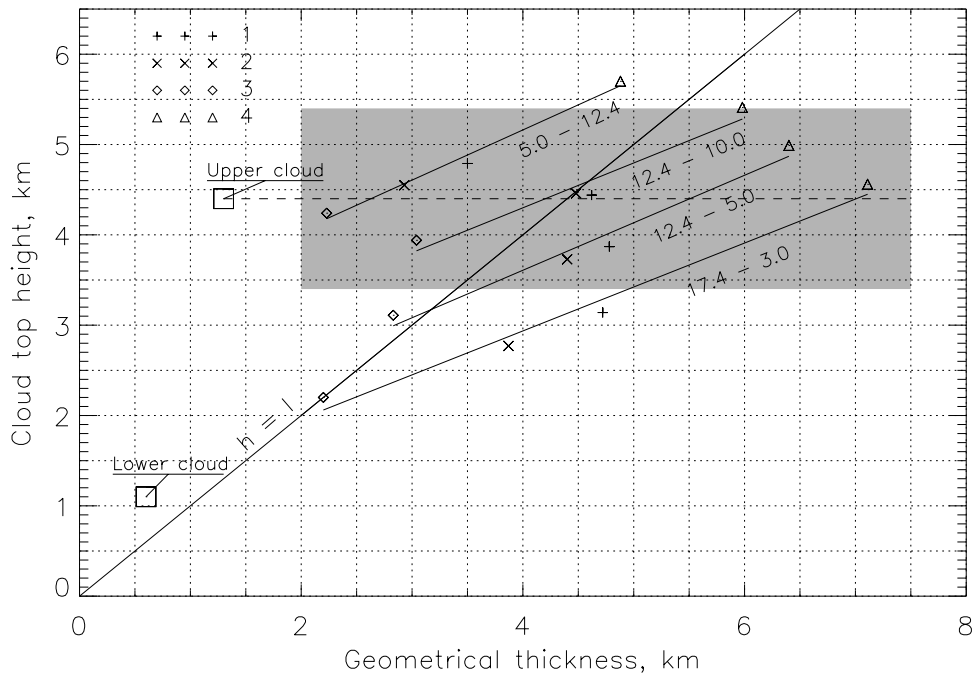

Figure 14. The same as in Figure 13 but $\mathbb{Z}$ = 2 km.

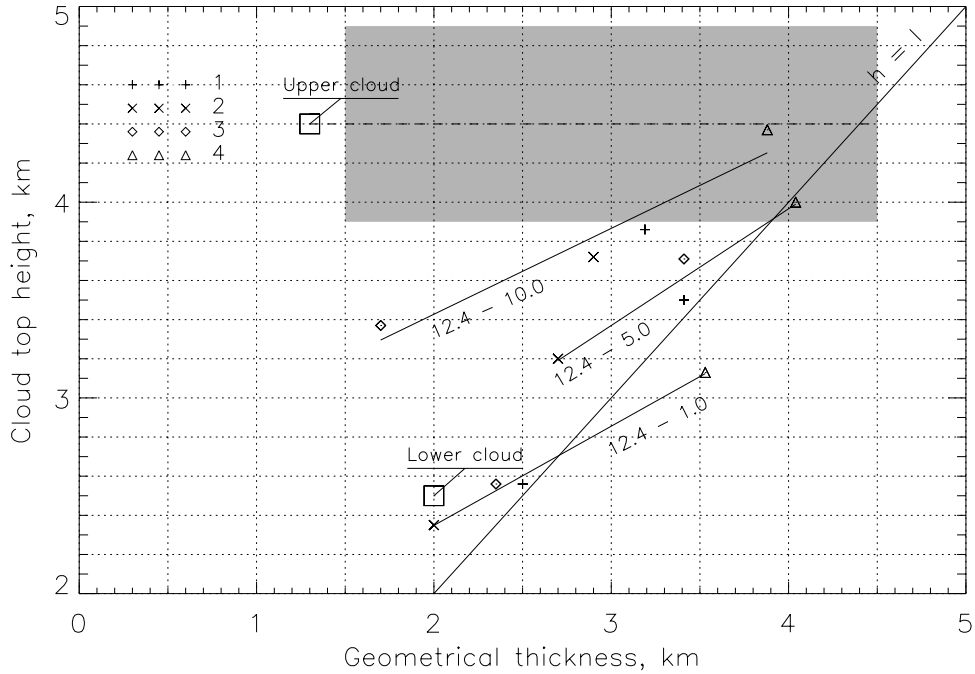

Figure 15. The results of the retrieval of h, l of the cloud system, composed of the upper ice cloud and lower water cloud. The distance between clouds $\mathbb{Z}$ is equal to 600 m. Other symbols have the same meaning as in Figure 13.

[93] 2. The geometrical thickness of the retrieved "effective" single cloud depends on the geometrical thickness of the layer between two clouds. The geometrical thickness of the retrieved "effective" cloud is equal to 4.3–4.8 km at $\mathbb{Z}$ = 600 m for considered cases (see Figure 13). This is close to the geometrical thickness of the layer between the cloud system top height and underlying surface. Interestingly, the value of l increases up to 6–7 km at $\mathbb{Z}$ = 2 km (see Figure 14). Then we have the unphysical condition $l > h$. This can be explained as follows. Namely, the cloud geometrical thickness determines the amount of light absorption in the cloud in the oxygen A band. Therefore the increase of $\mathbb{Z}$ leads to the increase of the absorption in the two-layered cloud system owing to the increase of amount of oxygen between cloud layers. This leads to the values of l larger than h. This unphysical result is due to the use of a single cloud with LWC = const in the retrieval procedure. In fact, the two-layered system should be used in the retrieval procedure. However, it is difficult to decide if a single cloud layer or a multilayered cloud system is responsible for a given TOA reflectance. By the way, if the retrieval gives $l > h$, then it is most probably that we have a multilayered case. Therefore our method can provide an indirect information on cloud system vertical structure. This by itself is a valuable information. Further research is needed in this direction, however.

[94] 3. The use of other types of the LWC profiles in the retrieval procedure for the two-layered case leads to systematically lower estimates of h and l as compared to results, obtained under assumption LWC = const. The difference reaches 1 and 2 km at $\mathbb{Z}$ = 600 m for h and l, respectively. It is even larger ($\approx$2.5 km) at $\mathbb{Z}$ = 2 km (see Figure 14).

[95] 4. The optical thickness τ^* of the two-layered system, retrieved using approach giving by *Kokhanovsky et al.* [2003], gives the value approximately equal to the sum of optical thicknesses of both layers.

[96] In conclusion, let us consider the results of the retrieval of parameters h and l with our algorithm, assuming the case of an ice cloud above liquid one. For this, we have created synthetic top of atmosphere reflectance data R_{mes} using SCIATRAN [*Rozanov et al.*, 2002] for this two-layered cloud system. The phase function of the ice cloud was modeled using the hexagonal prisms in according with the model of *Mishchenko et al.* [1999]. The height dependence of the phase function was neglected. Also, we have assumed that the vertical profile of the liquid/ice water content in both clouds correspond to the type 1, given in Figure 11.

[97] The results of retrievals assuming the single-layered liquid cloud system with LWC = const are given in Figures 15 and 16 at $\mathbb{Z}$ = 600 m and $\mathbb{Z}$ = 3.6 km, respectively. The optical thickness of the upper cloud layer was assumed to be between 1 and 10. Figures 15 and 16 are similar in many ways to Figures 13 and 14. This indicates that the thermodynamic state of the upper cloud influence the retrieval insignificantly. There are some differences, however. First of all, the crystalline clouds are usually optically thin. This leads to the increase of the retrieval error. In particular, the error is equal to $\sim$1.3 km at $\mathbb{Z}$ = 600 m and $\sim$2.5 km at $\mathbb{Z}$ = 3.6 km assuming a single cloud layer with LWC = const in the retrieval procedure.

[98] Second, the optical thickness of the retrieved cloud system τ is approximately two times larger than the sum of optical thicknesses of two separate cloud layers τ^* in this case. Remember that we had $\tau \approx \tau^*$ in the case of the liquid cloud system. The reason for this is that the existence of ice phase in the cloud is ignored in the retrieval procedure.

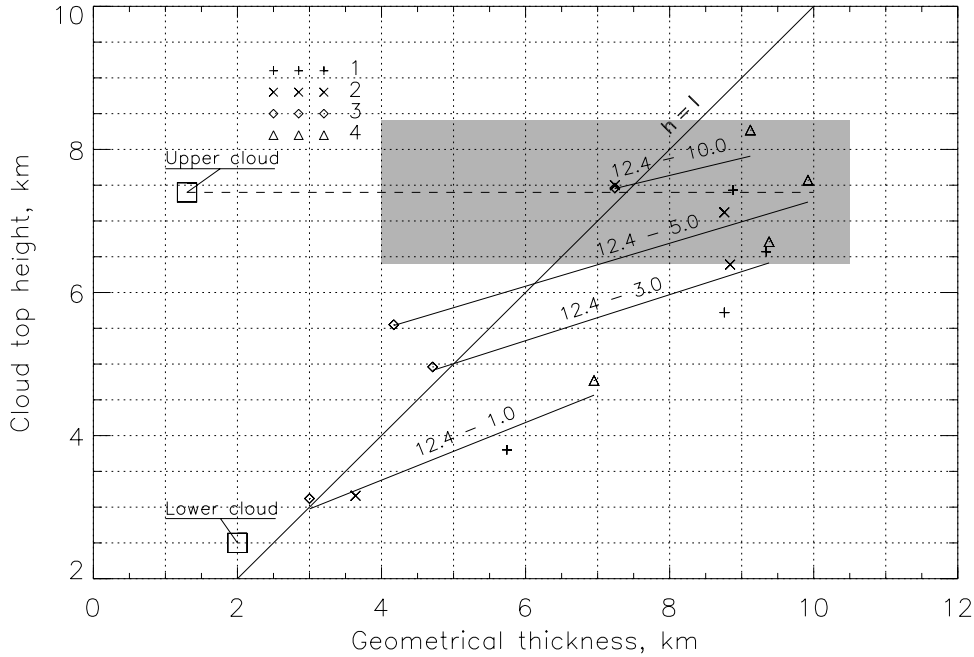

Figure 16. The same as in Figure 15, except at $\mathbb{Z}$ = 3.6 km.

Therefore the information on the cloud thermodynamic state is an essential for a correct run of the retrieval code.

5. Conclusion

[99] We presented here a simple and flexible asymptotic algorithm for the determination of cloud top height from measurements in the oxygen A band. Our technique can be also applied to other gaseous absorption bands. It relied on the semianalytical solution of the radiative transfer equation, which is valid for clouds having the cloud optical thickness larger than 5 [*Kokhanovsky and Rozanov*, 2003, 2004]. Note that thick clouds with $\tau > 5$ occur quite often [*Trishchenko et al.*, 2001]. The comparison of our algorithm with other retrieval methods is given in a separate publication [*Rozanov et al.*, 2004].

[100] The accuracy of the retrieval algorithm for the cloud top height determination if a single water cloud with LWC = const and known geometrical thickness is present in the scene under study is better than ~200 m. This error increases by ~50 m if the value of the cloud geometrical thickness is also unknown parameter. Then l can be also estimated. However, the error of the cloud geometrical thickness determination is generally larger (up to 3 times; see Figures 8 and 9) than that for the case of the cloud altitude determination.

[101] We also study the performance of our algorithm if a two-layered cloud system or a cloud with LWC $\neq$ const is present in the scene under study. Then errors of the retrieval increase considerably if a single cloud layer with the LWC = const is assumed in the retrieval procedure. Therefore it is of a great importance to select a right cloud model in the retrieval algorithm. This is a difficult problem, however, for measurements in real atmospheric conditions.

[102] Note that values of the cloud optical thickness, effective radius of droplets, and liquid water path can be found outside of the oxygen bands, using recently developed cloud retrieval algorithms [*Kokhanovsky et al.*, 2003; *Platnick et al.*, 2003], which are based on the similar assumptions as in the asymptotic algorithm described above.

[103] All studies presented above have been performed for the black underlying surface. The effects of polarization and non-plane-parallel geometry are neglected. The uncertainty of the ground reflectance (especially over land) can increase the retrieval error, so surface albedo databases should be used to avoid the problem. Our estimations (not presented here) show that the uncertainty in albedo of 50% (e.g., change of surface albedo from 0.2 to 0.3) results in 150 m (or smaller) error in the cloud top height determination if the cloud optical thickness is larger than 20. For thinner clouds the influence of incorrect albedo increases the retrieval error substantially. This confirms that accurate estimations of the surface albedo over land should be used as an input to our cloud retrieval algorithm. This problem is only of a minor importance for measurements over ocean.

[104] The combination of the cloud retrieval algorithm mentioned above [*Kokhanovsky et al.*, 2003] with that given in this paper allows to obtain a number of other cloud characteristics of interest (e.g., the liquid water content and cloud extinction coefficient) and constitutes a newly developed Semi-Analytical Cloud Retrieval Algorithm (SACURA). Note that the SACURA is much more faster and flexible than approaches based on the exact solution of the radiative transfer equation.

Appendix A: Auxiliary Functions

[105] Here we introduce without derivations auxiliary functions, which have been used in the main text of the paper (see Table 2). Details are given by *Kokhanovsky and Rozanov* [2003].

[106] Various parameters in Table 2 have the meaning described below [see also *Kokhanovsky and Rozanov*, 2003]. The value of $R^0_\infty(\xi, \eta, \varphi)$ gives us the reflection

Table 2. Auxiliary Functions [*Kokhanovsky and Rozanov* 2004; *Kokhanovsky et al.*, 2003]

Auxiliary Function	Formula
R_c	$R^0_\infty(\vartheta, \vartheta_0, \varphi)\exp(-y(1-0.05y)u(\vartheta, \vartheta_0, \varphi)) - t^* \exp(-x-y)K_0(\vartheta_0)K_0(\vartheta)$
u	$\frac{K_0(\vartheta)K_0(\vartheta_0)}{R^0_\infty(\vartheta,\vartheta_0,\varphi)}$
$K_0(\vartheta)$	$\frac{3}{7}(1+2\cos\vartheta)$
t^*	$t_c - (4.86-13.08\cos\vartheta_0\cos\vartheta + 12.76\cos^2\vartheta_0\cos^2\vartheta)\exp(x)/\tau^3$
t_c	$\frac{\sinh y}{\sinh[x+1.07y],}$
r_c	$\exp(-y(1-0.05y)) - t^*\exp(-x-y)$
r_a	$\omega_0\int_0^1 \xi d\xi \int_0^1 \eta d\eta F(\xi,\eta)\bar{p}(\xi,\eta)$
F	$\frac{1-\exp\left[-\tau^A\left(\xi^{-1}+\eta^{-1}\right)\right]}{\xi+\eta}$
R_a	$\frac{1}{4\xi\eta}\int_h^H dz(\sigma^R_{sca}(z)p^R(\theta) + \sigma^A_{sca}(z)p^A(z,\theta))\exp[-\tau(z)(\xi^{-1}+\eta^{-1})]$

function of a semi-infinite nonabsorbing cloud. It has the following simple form for close to nadir observations [*Kokhanovsky*, 2004]:

$$R^0_\infty(\zeta,\eta,\varphi) = \frac{A + B(\xi+\eta) + C\xi\eta + f(\theta)}{4(\xi+\eta)},$$

where $f(\theta) = p(\theta) - \bar{p}(\xi,\eta)$, $\theta = \arccos(-\xi\eta + \sqrt{(1-\xi^2)(1-\eta^2)}\cos\varphi)$, $\xi = \cos\vartheta_0$, $\eta = |\cos\vartheta|$, $\bar{p}(\xi,\eta) = \frac{1}{2\pi}\int_0^{2\pi} p(\theta)d\varphi$, and $A \approx 3.944$, $B \approx -2.5$, $C \approx 10.664$. Here $p(\theta)$ is the cloud phase function. The accuracy of this approximation is studied in detail by *Kokhanovsky* [2004].

[107] Parameters $x = yd$, $y = 4\sqrt{\frac{1-\omega_0}{3(1-g)}}$, $d = \frac{3}{4}(1-g)\tau_c$ are needed to describe the reflection function of a cloud at absorbing wavelengths. Here g is the asymmetry parameter [*Kokhanovsky*, 2001], ω_0 is the single scattering albedo, and τ_c is the cloud optical thickness.

[108] We found approximating the function $r_a(\tau^A)$ at the asymmetry parameter $g = 0.77$ and $\tau^A < 0.3$:

$$r_a(\tau) = 0.265\tau^A - 0.865\left(\tau^A\right)^2 + 1.164\left(\tau^A\right)^3,$$

where τ^A is the aerosol optical thickness beneath the cloud.

[109] Other parameters in Table 2 are defined as follows: (1) $\sigma^A_{sca}(z)$ and $\sigma^R_{sca}(z)$ are total aerosol and Rayleigh scattering coefficients, respectively; (2) $p^A(\theta, z)$ and $p^R(\theta)$ are aerosol and Rayleigh phase functions, respectively; (3) $\tau(z)$ is the optical depth of the atmosphere above z along the vertical axis OZ (see Figure 1), which includes the contribution from both molecular and aerosol scattering and absorption; and (4) H is the top of atmosphere height, assumed to be equal to 60 km in this study.

[110] The single scattering albedo ω_0 is defined by the following equation:

$$\omega_0 = 1 - \frac{\sigma_{\text{abs}}}{\sigma_{\text{ext}}},$$

where $\sigma_{\text{abs}} = \sigma^A_{\text{abs}} + \sigma^G_{\text{abs}} + \sigma^C_{\text{abs}}$ and $\sigma_{\text{ext}} = \sigma^A_{\text{ext}} + \sigma^G_{\text{ext}} + \sigma^C_{\text{ext}}$, where indices A, G, and C show aerosol, gas, or cloud contribution, respectively, to extinction σ_{ext} or absorption σ_{abs} coefficients.

[111] Let us assume that $\sigma^A_{\text{abs}} = \sigma^C_{\text{abs}} = 0$. Then we have

$$\omega_0 = 1 - \frac{\sigma^G_{\text{abs}}}{\sigma_{\text{ext}}}.$$

Thus the value of ω_0 changes with the height both inside and outside of a cloud. Formula for the cloud reflection in Table 2, however, is applicable only for the case of a vertically homogeneous layer. The dependence $\omega_0(z)$ is not particularly strong in the area, where cloud is present. Therefore we adopt here the model of an "effective homogeneous layer" [*Chamberlian*, 1965; *Yanovitskij*, 1997]. In this case one should find the height inside the cloud at which the value of ω_0 should be taken for calculations. Details of this are given by *Kokhanovsky and Rozanov* [2003]. Note that we also have accounted for the variation of the cloud liquid water content with the height.

[112] **Acknowledgments.** This work has been supported in part by the University of Bremen, the European Union Research Programme, the European Space Agency, the German Ministry of Research and Education (BMBF), and the German Space Agency (DLR). The authors are grateful to H. Bovensmann, M. Buchwitz, and J. P. Burrows for important discussions on the subject.

References

Asano, S., M. Shiobara, and A. Uchiyama (1995), Estimation of cloud physical parameters from airborne solar spectral reflectance measurements for stratocumulus clouds, *J. Atmos. Sci.*, *52*, 3556–3576.

Bezy, J. L., S. Delwart, and M. Rast (2000), MERIS—A new generation of ocean-colour sensor onboard ENVISAT, *ESA Bull.*, *103*, 48–56.

Bovensmann, H., J. P. Burrows, M. Buchwitz, J. Frerick, S. Noël, V. V. Rozanov, K. V. Chance, and A. P. H. Goede (1999), SCIAMACHY: Mission objectives and measurement modes, *J. Atmos. Sci.*, *56*, 127–150.

Buchwitz, M. (2000), Strahlungstransport- und Inversions- Algorithmen zur Ableitung Atmospharischer Spurengasinformationen aus Erdfernerkundungsmessungen in Nadirgeometrie im ultravioletten bis nahinfraroten Spektralbereich am Beispiel SCIAMACHY, Ph.D. thesis, Bremen Univ., Bremen.

Buchwitz, M., V. V. Rozanov, and J. P. Burrows (2000), A correlated-k distribution scheme for overlapping gases suitable for retrieval of atmospheric constituents from moderate resolution radiance measurements in the visible/near-infrared spectral region, *J. Geophys. Res.*, *105*, 15,247–15,262.

Burrows, J. P., et al. (1999), The Global Ozone Monitoring Experiment (GOME): Mission concept and first scientific results, *J. Atmos. Sci.*, *56*, 151–171.

Chamberlian, J. (1965), The atmosphere of Venus near her cloud tops, *Astrophys. J.*, *141*, 1184–1205.

de Beek, R., M. Vountas, V. V. Rozanov, A. Richter, and J. P. Burrows (2001), The ring effect in the cloudy atmosphere, *Geophys. Res. Lett.*, *28*, 721–724.

Deirmendjian, D. (1969), *Electromagnetic Scattering on Spherical Polydispersions*, Elsevier Sci., New York.

Feigelson, E. M. (Ed.) (1984), *Radiation in a Cloudy Atmosphere*, D. Reidel, Norwell, Mass.

Fischer, J., and H. Grassl (1991), Detection of cloud-top height from reflected radiances within the oxygen A band, part 1: Theoretical studies, *J. Appl. Meteorol.*, *30*, 1245–1259.

Fischer, J., et al. (1991), Detection of cloud-top height from reflected radiances within the oxygen A band, part 2: Measurements, *J. Appl. Meteorol.*, *30*, 1260–1267.

Fischer, J., L. Schuller, and R. Preusker (2000), Cloud top pressure, *MERIS Algorithm Theoretical Basis Doc. ATBD 2.3*, Free Univ. of Berlin, Berlin.

Gordon, H. R., D. K. Clark, J. W. Brown, O. B. Brown, R. H. Evans, and W. W. Broenkow (1983), Phytoplankton pigment concentrations in the Middle Atlantic Bight: Comparison of ship determination and CZCS estimates, *Appl. Opt.*, *22*, 20–36.

Grechko, E. I., V. I. Dianov-Klokov, and I. P. Malkov (1973), The airborne measurement of the effective photon free path lengths for light reflected and transmitted by clouds in the oxygen 0. 76 μm band, *Izv. Atmos. Oceanic Phys.*, *9*, 471–485.

Grechko, E. I., V. I. Dianov-Klokov, and I. P. Malkov (1975), The measurement of the effective photon free path length in cloud systems in situ, *Izv. Atmos. Oceanic Phys.*, *11*, 125–137.

Hagolle, O., P. P.-Y. Goloub, H. Deschamps, X. Cosnefroy, T. Briottet, T. Bailleul, J.-M. Nicolas, F. Parol, B. Lafrance, and M. Herman (1999), Results for POLDER in-flight calibration, *IEEE Trans. Geosci. Remote Sens.*, *37*, 1550–1566.

Hanel, R. A. (1961), Determination of a cloud altitude from a satellite, *J. Geophys. Res.*, *66*, 1300.

Hayasaka, T., T. Nakajima, Y. Fujiyoshi, Y. Ishizaka, T. Takeda, and M. Tanaka (1995), Geometrical thickness, liquid water content, and radiative properties of stratocumulus clouds over the western North Pacific, *J. Appl. Meteorol.*, *34*, 460–470.

Heidinger, A. K. (1998), Nadir sounding of clouds and aerosols in the A band of oxygen, Ph.D. thesis, Colo. St. Univ., Fort Collins, Colo.

Heidinger, A. K., and G. L. Stephens (2000), Molecular line absorption in a scattering atmosphere. part II: Application to remote sensing in O_2 A band, *J. Atmos. Sci.*, *57*, 1615–1634.

Heidinger, A. K., and G. L. Stephens (2002), Molecular line absorption in a scattering atmosphere. part III: Pathlength characteristics and effects of spatially heterogeneous clouds, *J. Atmos. Sci.*, *59*, 1641–1654.

Joiner, J., and P. K. Bhartia (1995), The determination of cloud pressures from rotational Raman scattering in satellite backscatter ultraviolet measurements, *J. Geophys. Res.*, *100*, 23,019–23,026.

King, M. D., Y. J. Kaufman, W. P. Menzel, and D. Tanre (1992), Remote sensing of cloud, aerosol, and water vapor properties from the moderate resolution imaging spectrometer (MODIS), *IEEE Trans. Geosci. Remote Sens.*, *30*, 2–27.

King, M. D., S.-C. Tsay, S. E. Platnick, M. Wang, and K.-N. Liou (1997), Cloud retrieval algorithms for MODIS: Optical thickness, effective particle radius, and thermodynamic state, *MODIS Algorithm Theoretical Basis Doc. ATBD-MOD-05*, NASA Goddard Space Flight Cent., Greenbelt, Md. (Available at http://ltpwww.gsfc.nasa.gov/MODIS-Atmosphere/_docs/atbd_mod05.pdf)

Knap, W. H., P. Stammes, and R. B. A. Koelemeijer (2002), Cloud thermodynamic phase determination from near-infrared spectra of reflected sunlight, *J. Atmos. Sci.*, *59*, 83–96.

Knibbe, W. J. J., J. F. de Haan, J. W. Hovenier, D. M. Stam, R. B. A. Koelemeijer, and P. Stammes (2000), Deriving terrestrial cloud top pressure from photopolarimetry of reflected light, *J. Quant. Spectrosc. Radiat. Transfer*, *64*, 173–199.

Kokhanovsky, A. A. (2001), *Light Scattering Media Optics: Problems and Solutions*, John Wiley, Hoboken, N. J.

Kokhanovsky, A. A. (2004), Reflection of light from nonabsorbing semiinfinite cloudy media: A simple approximation, *J. Quant. Spectoscr. Radiat. Transfer*, *85*, 25–33.

Kokhanovsky, A. A., and B. Mayer (2003), Light reflection and transmission by non-absorbing turbid slabs: simple approximations, *J. Opt. A Pure Appl. Opt.*, *5*, 43–46.

Kokhanovsky, A. A., and V. V. Rozanov (2003), The reflection function of optically thick weakly absorbing layers: a simple approximation, *J. Quant. Spectoscr. Radiat. Transfer*, *77*, 165–175.

Kokhanovsky, A. A., and V. V. Rozanov (2004), The physical parameterization of the top-of-atmosphere reflection function for a cloudy atmosphere—Underlying surface system: The oxygen A band case study, *J. Quant. Spectoscr. Radiat. Transfer*, *85*, 35–55.

Kokhanovsky, A. A., V. V. Rozanov, E. P. Zege, H. Bovensmann, and J. P. Burrows (2003), A semianalytical cloud retrieval algorithm using backscattered radiation in 0.4–2.4 μm spectral region, *J. Geophys. Res.*, *108*(D1), 4008, doi:10.1029/2001JD001543.

Kuang, Z., J. Margolis, G. Toon, D. Crisp, and Y. Yung (2002), Spaceborne measurements of atmospheric CO_2 by high-resolution NIR spectrometry of reflected sunlight: An introductory study, *Geophys. Res. Lett.*, *29*(15), 1716, doi:10.1029/2001GL014298.

Kuji, M., and T. Nakajima (2002), Retrieval of cloud geometrical parameters using remote sensing data, in *Proceedings of 11th Conference on Atmospheric Radiation* [CD-ROM], Am. Meteorol. Soc., Boston, Mass.

Lacis, A. A., and V. Oinas (1991), A description of the correlated k distribution method for modeling nongray gaseous absorption, thermal emission, and multiple scattering in vertically inhomogeneous atmospheres, *J. Geophys. Res.*, *96*, 9027–9063.

Li, Z. (2000), Accounting for overlap of fractional cloud in infrared radiation, *Q. J. R. Meteorol. Soc.*, *126*, 3325–3342.

Liou, K. N. (1992), *Radiation and Cloud Processes in the Atmosphere*, Oxford Univ. Press, New York.

Marchuk, G. I., K. Y. Kondratyev, V. V. Kozoderov, and V. I. Khvorostyanov (1986), *Clouds and Climate*, Gydrometeoizdat, St. Petersburg.

Mishchenko, M. I., J. M. Dlugach, E. G. Yanovitskij, and N. T. Zakharova (1999), Bidirectional reflectance of flat, optically thick particulate layers: An efficient radiative transfer solution and application to snow and soil surfaces, *J. Quant. Spectoscr. Radiat. Transfer*, *63*, 409–432.

Moroney, C., R. Davies, and J.-P. Muller (2002), Operational retrieval of cloud-top heights using MISR data, *IEEE Trans. Geosci. Remote Sens.*, *40*, 1532–1546.

Nakajima, T. Y. (2001), Development of a comprehensive analysis system for satellite measurement of the cloud microphysical properties, Ph.D. thesis, EORC NASDA, Tokyo.

Nakajima, D. T., and M. D. King (1990), Determination of the optical thickness and effective particle radius of clouds from reflected solar radiation measurements. part 1. Theory, *J. Atmos. Sci.*, *47*, 1878–1893.

Nakajima, T., M. D. King, J. D. Spinhirne, and L. F. Radke (1991), Determination of the optical thickness and effective particle radius of clouds from reflected solar radiation measurements. part II. Marine stratocumulus observations, *J. Atmos. Sci.*, *48*, 728–750.

Nakajima, T. Y., et al. (1998), Optimization of the Advanced Earth Observing Satellite, II, Global imager channels by use of the radiative transfer calculations, *Appl. Opt.*, *37*, 3149–3163.

Naud, C., J.-P. Muller, and E. E. Clothiaux (2002), Comparison of cloud top heights derived from MISR stereo and MODIS CO_2-slicing, *Geophys. Res. Lett.*, *29*(16), 1795, doi:10.1029/2002GL015460.

O'Brien, D. M., and R. M. Mitchell (1992), Error estimates for retrieval of cloud-top pressure using absorption in the A band of oxygen, *J. Appl. Meteorol.*, *31*, 1179–1192.

Platnick, S., M. D. King, S. A. Ackerman, W. P. Menzel, B. A. Baum, J. C. Riedi, and R. A. Frey (2003), The MODIS cloud products: Algorithms and examples from Terra, *IEEE Trans. Geosci. Remote Sens.*, *41*, 459–473.

Poole, L. R., D. M. Winker, J. R. Pelon, and M. P. McCormick (2003), CALIPSO: GLOBAL aerosol and cloud observations from lidar and passive instruments, *Proc. SPIE*, *4881*, 419–426.

Rodgers, C. (2000), *Inverse Methods for Atmospheric Sounding: Theory and Practice*, World Sci., River Edge, N. J.

Rothman, L. S., et al. (2003), The HITRAN molecular spectroscopic database: Edition of 2000 including updates through 2001, *J. Quant. Spectr. Radiat. Transfer*, *82*, 5–44.

Rozanov, V. V., T. Kurosu, and J. P. Burrows (1998), Retrieval of atmospheric constituents in the UV-visible: A new quasi-analytical approach for the calculation of weighting functions, *J. Quant. Spectr. Radiat. Transfer*, *60*, 277–299.

Rozanov, V. V., M. Buchwitz, K.-U. Eichmann, R. de Beek, and J. P. Burrows (2002), SCIATRAN—A new radiative transfer model for geophysical applications in the 240–2400 nm spectral range: The pseudo-spherical version, *Adv. Space Res.*, *29*, 1831–1835.

Rozanov, V. V., A. A. Kokhanovsky, and J. P. Burrows (2004), The determination of cloud top altitudes using GOME reflectance spectra: Multilayered cloud systems, *IEEE Geosci. Remote Sens.*, in press.

Saiedy, F. H., D. T. Hilleary, and W. A. Morgan (1965), Cloud-top altitude measurements from satellites, *Appl. Opt.*, *4*, 495–500.

Saiedy, F. H., H. Jacobowitz, and D. Wark (1967), On cloud-top determination from Gemini-5, *J. Atmos. Sci.*, *24*, 63–69.

Stephens, G. L., and A. K. Heidinger (2000), Molecular line absorption in a scattering atmosphere. part I: Theory, *J. Atmos. Sci.*, *57*, 1600–1614.

Stephens, G. L., and S.-C. Tsay (1990), On the cloud absorption anomaly, *Q. J. R. Meteorol. Soc.*, *116*, 671–704.

Thomas, G., and K. Stamnes (1999), *Radiative Transfer in the Atmosphere and Ocean*, Cambridge Univ. Press, New York.

Titov, G. (1998), Radiative horizontal transport and absorption in stratocumulus clouds, *J. Atmos. Sci.*, *55*, 2549–2560.

Trishchenko, A., Z. Li, and F.-L. Chang (2001), Cloud optical depth and TOA fluxes: Comparison between satellite and surface retrievals from multiple platforms, *Geophys. Res. Lett.*, *28*, 979–982.

Vanbauce, C., B. Cadet, and R. T. Marchand (2003), Comparison of POLDER apparent and corrected oxygen pressure to ARM/MMCR cloud boundary pressures, *Geophys. Res. Lett.*, *30*(5), 1212, doi:10.1029/2002GL016449.

van de Hulst, H. C. (1980), *Multiple Light Scattering: Tables, Formulas and Applications*, Academic, San Diego. Calif.

Wang, M., and M. D. King (1997), Correction of Rayleigh scattering effects in cloud optical thickness retrievals, *J. Geophys. Res.*, *102*(D22), 25,915–25,926.

Winker, D. M., et al. (1999), Global observations of aerosols and clouds from combined lidar and passive instruments to improve radiation budget and climate studies, in *Proceedings of the 10th Conference on Atmospheric Radiation*, pp. 290–293, Am. Meteorol. Soc., Boston, Mass.

Wiscombe, W., and G. W. Grams (1976), The backscattered fraction in two-stream approximations, *J. Atmos. Sci.*, *33*, 2440–2451.

Wrigley, R. C., M. A. Spanner, R. E. Slye, R. F. Pueschel, and H. R. Aggarwal (1992), Atmospheric correction of remotely sensed image data by a simplified model, *J. Geophys. Res.*, *97*(D17), 18,797–18,814.

Wu, M.-L. C. (1985), Remote sensing of cloud-top pressure using reflected solar radiation in the oxygen A band, *J. Clim. Appl. Meteorol.*, *24*, 539–546.

Yamomoto, G., and D. Q. Wark (1961), Discussion of letter by A. Hanel: Determination of cloud altitude from a satellite, *J. Geophys. Res.*, *66*, 3596.

Yanovitskij, E. G. (1997), *Light Scattering in Inhomogeneous Atmospheres*, Springer-Verlag, New York.

A. A. Kokhanovsky and V. V. Rozanov, Institute of Environmental Physics, Bremen University, P.O. Box 330440, Bremen D-28334, Germany. (alexk@iup.physik.uni-bremen.de)